[redacted]

CENTRAL RESEARCH LIBRARY
DOCUMENT COLLECTION

Inv 55

CLASSIFICATION CHANGED TO: Declassified
BY AUTHORITY OF: T.I.D. 1112
BY: K. Page 10/26/56

ORNL 1583
Reactors-Research and Power

Inv 55

MARTIN MARIETTA ENERGY SYSTEMS LIBRARIES
3 4456 0060725 2

DEVELOPMENT OF HYDROGEN-OXYGEN RECOMBINERS

PROGRESS REPORT

J. A. Ransohoff
I. Spiewak

OAK RIDGE NATIONAL LABORATORY
CENTRAL RESEARCH LIBRARY
CIRCULATION SECTION
4500N ROOM 175
LIBRARY LOAN COPY
DO NOT TRANSFER TO ANOTHER PERSON
If you wish someone else to see this report, send in name with report and the library will arrange a loan.
UCN-7969 (3 9-77)

OAK RIDGE NATIONAL LABORATORY
OPERATED BY
CARBIDE AND CARBON CHEMICALS COMPANY
A DIVISION OF UNION CARBIDE AND CARBON CORPORATION
UCC
POST OFFICE BOX P
OAK RIDGE, TENNESSEE

[redacted]

[redacted]

[redacted]

ORNL-1583

[redacted]

Contract No. W-7405, Eng 26

Reactor Experimental Engineering Division

DEVELOPMENT OF HYDROGEN-OXYGEN RECOMBINERS

PROGRESS REPORT

by

J. A. Ransohoff

and

Irving Spiewak

Date Issued

OCT 12 1953

OAK RIDGE NATIONAL LABORATORY
Operated by
CARBIDE AND CARBON CHEMICALS DIVISION
Union Carbide and Carbon Corporation
Post Office Box P
Oak Ridge, Tennessee

[redacted]

[redacted]

ORNL 1583
Reactors-Research
and Power

INTERNAL DISTRIBUTION

1. C. E. Center
2. Biology Library
3. Health Physics Library
4-5. Central Research Library
6. Reactor Experimental Engineering Library
7-12. Laboratory Records Department
13. Laboratory Records, ORNL R.C.
14. C. [illegible] Lind
15. W. [illegible] Ames (K-25)
16. L. [illegible] Amer (Y-12)
17. A. M. [illegible]erg
18. E. [illegible] Taylor
19. E. [illegible] Shelley
20. C. [illegible] Winters
21. [illegible] VoorhierLage
22. [illegible] Grant
23. [illegible] Swartout
24. S. C. Lind
25. F. [illegible] Culler
26. A. [illegible] Snell
27. A. Hollaender
28. M. T. Kelley
29. W. J. Fretague
30. G. H. Clewett
31. K. Z. Morgan
32. T. A. Lincoln
33. A. S. Householder
34. C. S. [illegible]
35. D. S. [illegible]ington
36. D. [illegible] Cardwell
37. E. [illegible] King
38. R. N. [illegible]
39. J. A. [illegible]
40. A. [illegible] Miller
41. R. [illegible] Briggs
42. A. S. [illegible]zes
43. [illegible] Sisman
44. R. [illegible] Stoughton
45. C. [illegible] Graham
46. W. R. Gill
47. [illegible] Koppendiek
48. S. [illegible] Beall
49. J. [illegible] Gill
50. D. [illegible] Cowen
51. W. M. Breazeale (consultant)
52. R. A. Charpie
53. R. H. Wilson
54. I. Spiewak
55. R. E. Aven

EXTERNAL DISTRIBUTION

56. AF Plant Representative, Burbank
57. AF Plant Representative, Seattle
58. AF Plant Representative, Wood-Ridge
59. ANP Project Office, Fort Worth
60-70. Argonne National Laboratory
71. Armed Forces Special Weapons Project (Sandia)
72-76. Atomic Energy Commission, Washington
77. Battelle Memorial Institute
78. Bechtel Corporation
79-81. Brookhaven National Laboratory
82. Bureau of Ships
83-84. California Research and Development Company
85-90. Carbide and Carbon Chemicals Company (Y-12 Plant)
91. Chicago Patent Group
92. Chief of Naval Research
93. Commonwealth Edison Company
94. Department of the Navy - Op-362
95. Detroit Edison Company

[redacted]

[redacted]

96-99. duPont Company, Augusta
100. duPont Company, Wilmington
101. Foster Wheeler Corporation
102-104. General Electric Company (ANPP)
105-108. General Electric Company, Richland
109. Hanford Operations Office
110-116. Idaho Operations Office
117. Iowa State College
118-121. Knolls Atomic Power Laboratory
122-123. Los Alamos Scientific Laboratory
124. Massachusetts Institute of Technology (Kaufmann)
125. Monsanto Chemical Company
126. Mound Laboratory
127. National Advisory Committee for Aeronautics, Cleveland
128. National Advisory Committee for Aeronautics, Washington
129. Naval Research Laboratory
130-131. New York Operations Office
132-133. North American Aviation, Inc.
134. Nuclear Development Associates, Inc.
135. Patent Branch, Washington
136. Powerplant Laboratory (WADC)
137. Pratt and Whitney Aircraft Division (Fox Project)
138. Rand Corporation
139. San Francisco Operations Office
140. Savannah River Operations Office, Augusta
141. USAF Headquarters
142. U. S. Naval Radiological Defense Laboratory
143-144. University of California Radiation Laboratory, Berkeley
145-146. University of California Radiation Laboratory, Livermore
147. Vitro Corporation of America
148. Walter Kidde Nuclear Laboratories, Inc.
149-154. Westinghouse Electric Corporation
155-169. Technical Information Service, Oak Ridge
170. Pioneer Service and Engineering Company

[redacted]

TABLE OF CONTENTS

CHAPTER		PAGE
I.	THE TESTING AND OPERATION OF FLAME AND CATALYTIC RECOMBINERS ON THE HOMOGENEOUS REACTOR EXPERIMENT	8
	Summary	8
	Description of the Off-Gas System	8
	Recombiner Details	11
	Catalytic Recombiners	11
	Flame Recombiner	13
	Testing of the Recombiners	15
	D_2O System Recombiners	15
	Fuel Catalytic Recombiner	16
	Flame Recombiner	16
	Flashback Testing	17
	Recombiner Operation	19
	D_2O Recombiners	19
	Fuel Catalytic Recombiner	20
	Flame Recombiner	20
	Estimated Gas Production in the HRE	22
	Acknowledgments	22

[redacted]

[redacted]

[redacted]

TABLE OF CONTENTS (CONT'D)

CHAPTER		PAGE
II.	THE CATALYTIC REACTION OF $2H_2 + O_2$ ON PLATINIZED ALUMINA	24
	Summary	24
	Introduction	24
	The Apparatus	25
	Discussion of Results	29
	Reliability and Possible Sources of Error	44
	Conclusions	45
	Future Plans and Recommendations	46
III.	THE DEVELOPMENT OF AN EXPLOSION PROOF, AUTOMATIC LOAD ADJUSTING, FLAME RECOMBINER	48
	Summary	48
	Introduction	48
	The Apparatus	49
	Operating Characteristics	52
	Conclusions	56
	Acknowledgments	56
APPENDIX A.	A Catalytic Combustion Hydrogen Gas Analyser	57
APPENDIX B.	Derivation of the Equation Relating Recombination Efficiency to Hydrogen-Oxygen Ratio	64
APPENDIX C.	Theoretical Calculation of Recombination with Diffusion Controlling	67
APPENDIX D.	Table of Observed Mass Transfer Coefficeints	70
APPENDIX E.	Summary of Observed and Calculated Data	72

[redacted]

[redacted]

TABLE OF CONTENTS (CONT'D)

LIST OF FIGURES

		PAGE
1	HRE Off-gas System	9
2	HRE Catalytic Recombiner	12
3	HRE Flame Recombiner	14
4	Gas Production in the HRE	23
5	Test Catalytic Recombiner Flow Diagram	26
6	Catalytic Recombiner	27
7	Recombiner Efficinecy vs. Oxygen to Hydrogen Ratio	29
8	Typical Plot of $\frac{O_o}{2O_o - H_o}$ vs. $\frac{H_f}{2O_o - H_o}$	31
9	Typical Plot of $\frac{O_o}{2O_o - H_o}$ vs. $\frac{H_f}{2O_o - H_o}$ at 231°C	34
10	Typical Plot of $\frac{O_o}{2O_o - H_o}$ vs. $\frac{H_f}{2O_o - H_o}$ at 437°C	35
11	Typical Plot of $\frac{O_o}{2O_o - H_o}$ vs. $\frac{H_f}{2O_o - H_o}$ at 432°C	36
12	Typical Plot of $\frac{O_o}{2O_o - H_o}$ vs. $\frac{H_f}{2O_o - H_o}$ at 515°C	37
13	Hydrogen Mass Transfer Coefficients as a Function of Temperature and Pressure	39
14	Hydrogen Mass Transfer Coefficients as a Function of Flow Rate	40
15	Comparison of Hydrogen and Deuterium Data	43
16	Experimental Flame Recombiner Flowsheet	50

[redacted]

[redacted]

TABLE OF CONTENTS (CONT'D)

LIST OF FIGURES

		PAGE
17	Experimental Flame Recombiner	51
18	Flame Recombiner Temperature vs. Gas Flow Rate	55
19	Sensing Cell and Cell Block for a Catalytic Recombiner H_2 System	58
20	Schematic Diagram of the Analyzer Sampling System	59
21	Schematic Diagram of the Heater Current Control	60
22	A Typical Analyzer Calibration Curve	62

[redacted]

[redacted]

DEVELOPMENT OF HYDROGEN-OXYGEN RECOMBINERS

During the past year there have been several developments in the recombiner field which should be of interest to those concerned with homogeneous reactor technology. It is the purpose of this report to review our experience with recombiners under actual reactor operating conditions, and to discuss new developments in the field. This end can best be accomplished by reporting our work in three somewhat independent chapters, each of which shall be a report in itself:

Chapter I	-	The testing and operation of flame and catalytic recombiners in the ORNL Homogeneous Reactor Experiment - by J. A. Ransohoff
Chapter II	-	The effect of oxygen concentration, temperature, pressure, and space velocity on catalytic recombination by platinized alumina - by J. A. Ransohoff and I. Spiewak
Chapter III	-	The development of a flashback-proof, automatic load adjusting flame recombiner, mainly for use on a boiling reactor - by J. A. Ransohoff and I. Spiewak.

J. A. Ransohoff

I. Spiewak

[redacted]

CHAPTER I

THE TESTING AND OPERATION OF FLAME AND CATALYTIC RECOMBINERS ON THE HOMOGENEOUS REACTOR EXPERIMENT

Summary

It is estimated that the HRE produces 10 cfm (STP) of $2H_2 + O_2$ per megawatt during power operation. There is no evidence that any of the combustible gas produced in the reactor escapes unrecombined. In this section we will describe the off-gas system, and discuss the preliminary testing of the recombiners, the performance of the recombiners under operating conditions, and the reliability of our gas production estimates.

Description of the Off-Gas System

The HRE was expected to produce 11.3 cfm* (STP) of $2H_2 + O_2$ per megawatt of reactor power. Since the operating level may be set at any fraction of that power for prolonged periods of time, the gas handling system was designed to handle all gas quantities between zero and 15 cfm. A simplified flow diagram of the HRE off-gas system is shown in Figure 1.

---

* T. J. Sworski (p.117, HRP Quarterly Report, Jan. 1, 1953, ORNL-1478, Uranyl Sensitized Reaction of H_2 and O_2) has developed an equation to be used in predicting the amount of gas produced in aqueous homogeneous reactors. For UO_2SO_4 solutions it is:

$$g = 1.83 - 0.0488(C)^{1/2}$$

where..... g = molecules H_2 formed per 100 ev of fission energy

C = concentration of U (total) in solution--- gms of UO_2SO_4/liter

For mean operating conditions in the HRE on Feb. 23-24, the predicted "g" value using Sworski's equation was 1.53, and the predicted gas production 11.3 cfm (STP) per megawatt of reactor power.

[redacted]
Dwg. 18098 R1

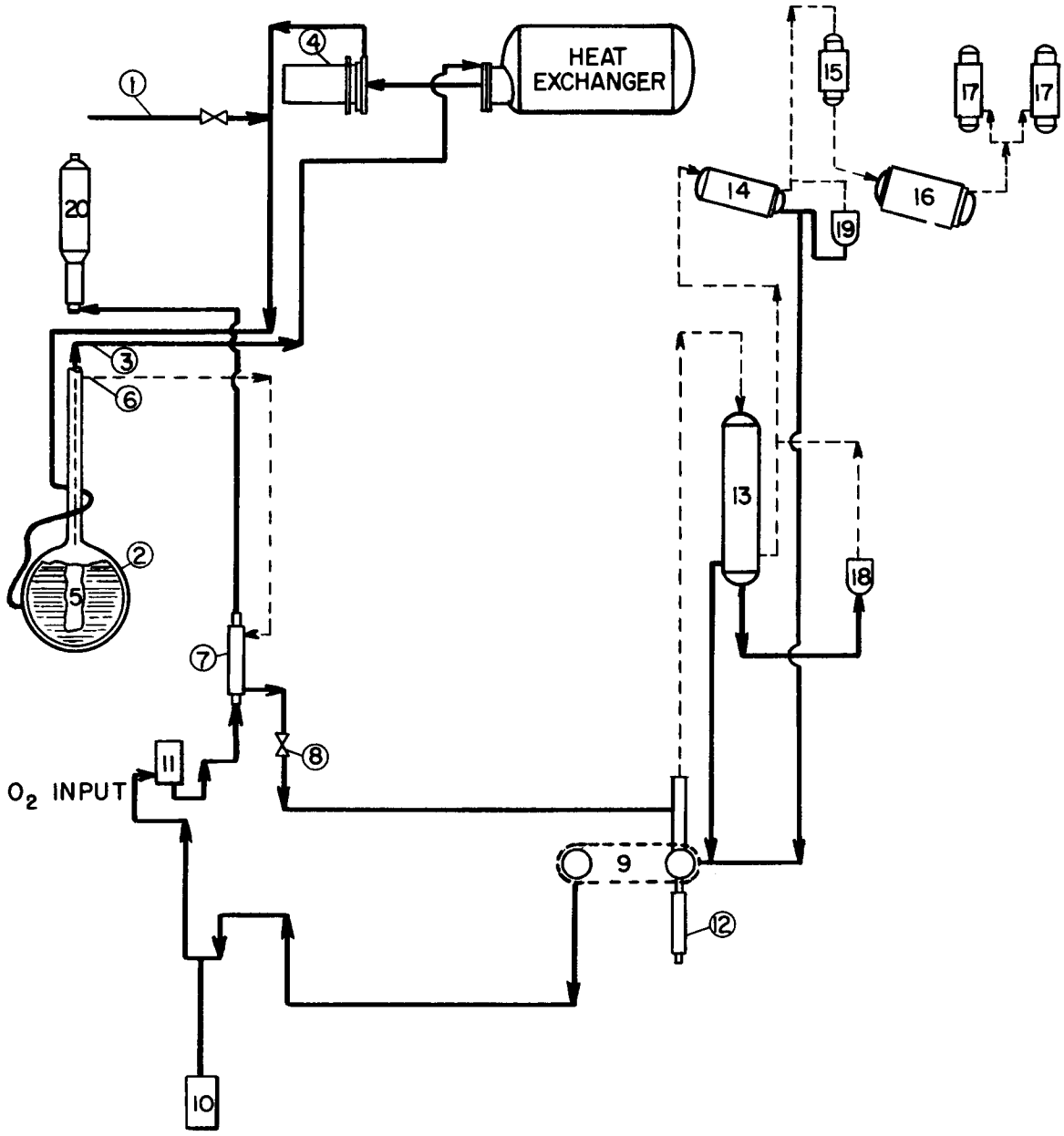

1. STOICHIOMETRIC GAS INLET
2. CORE
3. SECOND OF 3 CONCENTRIC PIPES
4. CANNED ROTOR CENTRIFUGAL PUMP
5. VORTEX
6. THIRD OF 3 CONCENTRIC PIPES
7. DOUBLE PIPE HEAT EXCHANGER
8. LETDOWN VALVE
9. DUMP TANKS
10. PULSAFEEDER
11. OXYGEN ABSORBER
12. FUEL EVAPORATOR
13. FORE CONDENSER
14. FLAME RECOMBINER
15. CATALYTIC RECOMBINER
16. AFTER CONDENSER
17. COLD TRAPS
18. STEAMER POT
19. STEAMER POT
20. PRESSURIZER

FIGURE 1

HRE OFF-GAS SYSTEM

The gas formed in the fuel solution at pressures up to 1000 psi and temperatures up to 250°C is removed from solution, let down to atmospheric pressure, recombined to water, and returned as such to the fuel solution. The gas, along with some steam and fuel solution, is throttled through a valve (8) into the dump tanks (9) where an evaporator (12) adds up to 40 cfm (STP) of steam to the gas so that the mixture flowing from the dump tanks to the recombiner system is noncombustible.*,** The steam is condensed from the gas in a large condenser (13), making the mixture once again combustible; and the condensate is either returned by gravity to the dump tanks, or is collected in condensate weigh tanks if it is desired to concentrate the fuel solution.

The gases then flow from the condenser to the flame recombiner (14) where the H_2 and O_2 are burned to water, most of which is condensed in the combustion chamber which is a 3 1/2 foot length of 10 inch pipe, jacketed by a 12 inch pipe through which cooling water is circulated. At extremely low power levels (less than 20 kw), operation of the flame recombiner is erratic, and overall recombiner operations are improved if the spark is shut off and the gases are allowed to flow into the catalytic recombiner (15) where the H_2-O_2 reaction is catalysed by 1/8 inch platinized alumina pellets. Following the catalytic recombiner is another condenser (16) in which most of the remaining water vapor is condensed. The gases still remaining (fission products plus 1200 cc/min. of O_2 that are continually bled into the system at (11)), then pass through cold

---

* D. W. Kuhn et al, Explosion Limits in Mixtures of H_2 and O_2, Steam and He, Oak Ridge National Laboratory, Y-731, 1951. Secret.

** H. M. McLeod et al, Recombination of Stoichiometric Mixtures of H_2 and O_2 in a Flame Recombiner (Feasibility Report), Oak Ridge National Laboratory, Y-706, 1951. Secret.

traps (17) where last traces of water vapor are removed from the gas. Before the O_2 is released to atmosphere, it is stripped of accompanying fission products by being passed through a charcoal bed. The condensed products of combustion are returned to the fuel in the dump tanks by gravity.

In addition to the gases produced in the fuel solution, it was expected that up to 1/4 cfm of $2D_2 + O_2$ would be produced by decomposition of D_2O in the reflector. Accordingly, the He used to pressurize the reflector is circulated through a catalytic recombiner placed in the high pressure D_2O gas system. The gas circulation is accomplished by use of a liquid-gas jet placed in the D_2O circulation line, and the recirculated gas returns to the reflector vessel along with the liquid. To provide for a means of handling the decomposed gas in the event of a reflector dump or He bleedoff, a catalytic recombiner is also placed in the low pressure D_2O system.

Recombiner Details

Catalytic Recombiners

All of the catalytic recombiners on the HRE are essentially the same as that shown in Figure 2. Unless the gases passing through the catalytic recombiners have a low enough H_2 concentration so that the mixture is non-combustible, an explosion is likely to result.

There is enough He in the reflector vessel, and the velocity with which it is circulated is sufficiently high to adequately dilute the radiolytic $D_2 + O_2$ formed in the reflector. Whatever gases flow into the low-pressure catalytic recombiner in the fuel system are first diluted by up to 3 cfm (STP) of steam produced by a small evaporator (19) placed between the flame and catalytic recombiners. This quantity of steam is more than enough to dilute

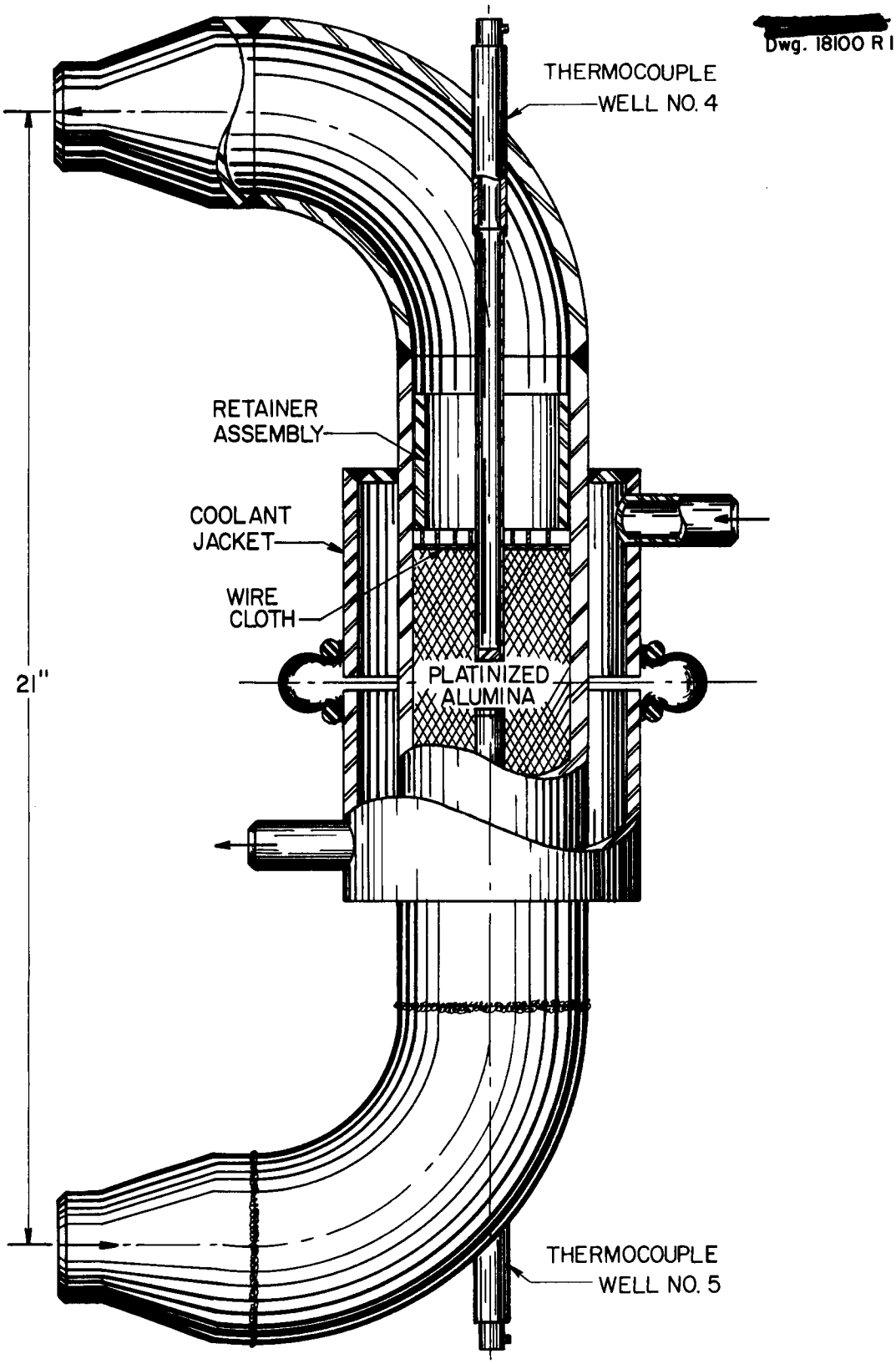

FIGURE 2

HRE CATALYTIC RECOMBINER

the 1/4 cfm of $2H_2 + O_2$ that the catalytic recombiner is expected to handle at maximum load.

The catalyst may be poisoned by either a liquid film of water or a layer of adsorbed I_2. Protection from "water poisoning" is provided by jacketing the recombiners with high-pressure steam which serves to keep the catalyst dry. It is now believed that the I_2 produced by fission in an O_2 rich fuel solution will be oxidized to IO_3^-, and if this be the case, no precaution against poisoning need be taken. If molecular I_2 is produced however, the catalyst may be cleansed of I_2 by occasionally heating the bed to about 400°C with the hot gases produced in the flame recombiner during relatively high power operation.

Flame Recombiner

The flame is established at a many-holed nozzle upon which a spark impinges from one of three spark plugs located along the periphery of the nozzle (see Figure 3). The spark impulse is produced by a magneto, and an ignition transformer is held in standby in case of magneto failure.

The flow area of the nozzle consists of 147 holes 1/32 inch in diameter, the total cross section being 0.112 sq. in. When the flow rate through the nozzle reaches 25 cfm of reactor gas, the velocity through the nozzle becomes 640 feet/sec., and the pressure drop through the nozzle approaches the 11 foot water head by which the condensate is returned to the dump tanks. At flows of less than three cfm, the pressure drop across the nozzle is so low that the flame burns too close to the tip, the nozzle overheats, and flashbacks result.

[redacted]
Dwg. 18099 R1

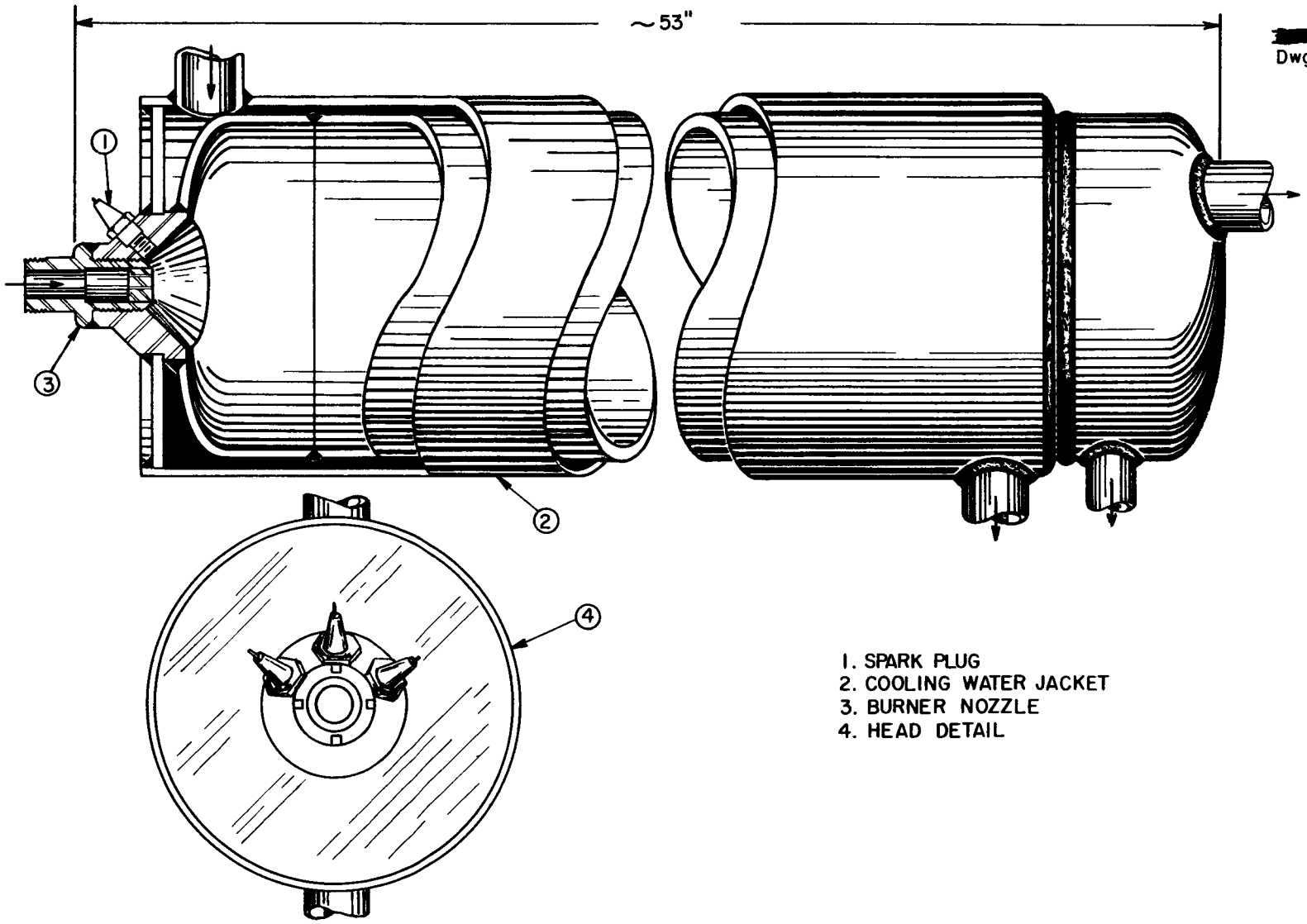

1. SPARK PLUG
2. COOLING WATER JACKET
3. BURNER NOZZLE
4. HEAD DETAIL

FIGURE 3

HRE FLAME RECOMBINER

To prevent flashbacks at low power levels, a steamer pot (18) provides 2 to 3 cfm (STP) of steam to the gas stream flowing from the fore condenser to the recombiner. The steam produced serves both to cool the flame by dilution, and to provide the minimum flow necessary to keep the flame from burning directly on the nozzle. The spark is operated continuously at all times to insure constant burning of the gas, although at flows of greater than 2 cfm a stable flame is established.

Testing of the Recombiners

D_2O System Recombiners

The low pressure D_2O catalytic recombiner was tested by passing electrolytic $2H_2 + O_2$, diluted with He, through the D_2O low pressure system, and observing the temperature rise in the catalyst. No extensive quantitative data was taken, but a flow of 4 cfm of He with 2 percent H_2 increased 70°C in temperature while flowing through the bed, and this was accepted as sufficient proof that the overdesigned bed would serve its function.

The high pressure D_2O recombiner was tested with water in the reflector vessel at 200°C and circulating, and enough He in the system to bring the total pressure to 650 psi. H_2 and O_2 were added in nearly stoichiometric amounts from high pressure cylinders. The results are expressed below in terms of equilibrium recombiner temperatures:

[redacted]

Reflector Temperature °C	Reflector Pressure psi	Gas Admitted cfm (STP) $2H_2+O_2$	Equilibrium Recombiner Temperature °C
197	650	0.0	200
196	625	0.33	286
197	653	0.42	360

Fuel Catalytic Recombiner

To test the fuel catalytic recombiner, electrolytic gas was admitted to the low pressure fuel system, and allowed to flow through the recombiners with the spark turned off and both steamer pots producing approximately 2.5 cfm of steam. Operation was satisfactory.

The Data

Gas Admitted cfm (STP) $2H_2 + O_2$	Recombiner Temp. °C t.c. No.4	t.c. No.5
0.0	115	115
0.22	270	210
0.10	208	165

Flame Recombiner

The flame recombiner on the HRE was operated at flows varying from less than 1/4 to more than 15 cfm (STP) of $2H_2 + O_2$ prior to power operation of the reactor. It was discovered during this operation that the fuel off-gas recording apparatus was not entirely reliable, and it was decided to make a heat balance across the recombiner system to see if off-gas flow could be determined accurately in that manner. From the data taken (see table below), it was agreed that heat balance determination of off-gas flow rate would be accurate to within 5 or 10 percent.

The Data

Gas Flow cfm at STP H_2	O_2	Heat Balance (BTU/Min.) A In with Gas	B Out with Cooling Water	Percent Difference (A-B)/B
1.67	0.80	544	541	0.6
2.58	1.40	877	805	8.9
3.3	1.60	1090	974	11.9
2.35	1.27	780	793	1.6
5.0	2.45	1670	1394	19.8
4.3	2.0	1362	1322	3.0
5.0	2.46	1675	1545	8.5
6.4	3.1	2110	1953	8.0
6.2	4.0	2110	2313	-8.7
Excess	0.68	464	499	-7.0
Excess	0.60	409	427	-4.3
7.1	3.6	2410	2404	0.3
7.7	3.7	2520	2404	4.8
5.3	2.45	1670	1773	-5.8
2.6	1.22	832	853	-2.5
5.7	2.67	1816	1720	5.6
6.8	3.1	2110	1977	6.7
9.5	4.3	2930	2640	11.0
3.4	1.72	1152	1080	6.7

There is an inherent error of about five percent due to variations in cooling water flow, and an error of a percent or two in gas flow measurement through the calibrated orifices used for these tests. Errors that might be caused by conditions in the off-gas cell and general heat losses and gains due to irrelevant factors were accounted for by using as "zero" temperature the temperature of the exit cooling water when no H_2 was flowing.

Flashback Testing

Flashbacks originating in the recombiner system create peak pressures of from 100 to 400 psi depending on the starting pressure and the H_2-O_2 concentration.*

---

* T. H. Pigford, Explosion and Detonation Properties of Mixtures of H_2 and O_2 and Water Vapor, Oak Ridge National Laboratory, ORNL-1322, 1952. [redacted]

Such explosions will be quenched in the line between the dump tanks and the fore condenser, or in the condenser itself, if the gas mixture contains more than 70% steam*. There is, of course, a possibility that the process solution evaporator (12) may fail or be turned off for some reason, or that gas flows much greater than expected will have to be handled. It was feared that if the mixture in the off-gas line were combustible, an explosion originating in one of the recombiners might travel back through the off-gas line to the dump tanks and thence through the let-down valve into the high-pressure system.

To see whether or not this would be the case, H_2 and O_2 were admitted to water circulating in the high pressure system at (1) with that system operating at 250°C and 1000 psi. The gases then flowed with the water into the core (2) where the circulatory motion of the liquid set up a gas vortex (5). From the vortex, the mixture of H_2, O_2, steam and water passed through the let-down heat exchanger (7) and valve (8) into the low pressure system where the gas was allowed to pass undiluted to the recombiners. The liquid taken from the core was replaced by pumping water from the dump tanks back into the core with a pulsafeeder (10).

---

* H. M. McLeod et al, Recombination of Stoichiometric Mixtures of H_2 and O_2 in a Flame Recombiner (Feasibility Report), Oak Ridge National Laboratory, Y-706, 1951. [redacted]

The sparks in the flame recombiner were left off, and when the combustible gas came in contact with the catalyst, flashbacks resulted. With a gas flow of 8 cfm, it was immediately evident that the flashbacks were travelling all the way to the dump tanks. However, when the gas flow was increased to 12 cfm, the flashbacks, which had been occurring every ten seconds, increased in frequency to about once every 6 or 7 seconds, and then ceased. Concurrently the temperature in the line connecting the dump tanks and the recombiner system rose sharply, and the gas was immediately turned off.

Apparently a flame had become established somewhere between the let-down valve and the line leading from the dump tanks, but we were satisfied that an explosion originating in the recombiners would not travel back up through the let-down valve into the high pressure system at design temperature and pressure.

Recombiner Operation

On February 20, 23, 24, and March 18, the HRE was operated at power levels high enough to learn something about the operation of the recombiners under actual power operating conditions. The following observations were made:

D_2O Recombiners

No decisive temperature increase in either of the D_2O recombiners was observed. However, it would require a considerable period of high-power

operation to effect a very large increase in D_2 - O_2 concentration in the He diluent, and there is no reason to suspect the recombiners of being ineffective; so no conclusions can yet be drawn.

Fuel Catalytic Recombiner

The spark to the flame recombiner was left off during power operation of the reactor at 10 and 20 kw, and the catalytic recombiner was allowed to recombine the gas produced, which it did nicely. Some buildup in pressure was observed during this operation, but it is believed that this was due to frozen cold traps which did not allow the excess O_2 to escape; rather than incomplete recombination.

Flame Recombiner

Minor flashbacks which could best be described as mild pressure surges were observed in varying degree from the point at which the flame recombiner was put into use (varied from 0 to 40 kw) up to power levels of 200 kw. From about 150 to 300 kw reactor power, there is a transitional range in which burning is relatively smooth but is accompanied by a rather shrill whistle. At power levels above 300 kw, burning is extremely smooth and is unaccompanied by noise of any kind. As the reactor power is increased much above 1 Mw, the pressure drop through the recombiner nozzle becomes such that it is difficult to keep the pressure in the fore condenser below 1 atmosphere as is desired because of a leak in the condenser. It was found that shutting off the steamer pot directly before the recombiner reduced the mass rate of flow and the gas temperature to a point where the condenser pressure was no longer excessive.

It is possible, however, to reach a reactor power* where so much gas is produced that the temperature (at the base) of the recombiner exceeds 600 °C, a temperature considered too high for safe long term operation. This is probably the limiting factor in determining maximum permissible operating power of the present HRE.

---

* During the high power run of March 18, the thermocouple at the base of the flame recombiner read 610 °C at which point the reactor power was reduced. The nuclear instruments read 1480 kw at the power level corresponding to the recombiner temperature mentioned above. At that power approximately 15 cfm of $2H_2 + O_2$ should be produced (by extrapolating the data obtained on February 23-24). The power was not maintained long enough to determine the amount of gas produced, but during pre-power tests on the recombiners, flows of 15.6 and 13.2 cfm were established long enough to obtain reliable data. The corresponding temperatures at the base of the recombiner were 480 °C and 575 °C, so it seems probable that about 16 cfm were being burned in the recombiner during the run of March 18, and that the reactor power was probably much nearer to 1600 than 1500 kw. This contention is not weakened by an admission on the part of the nuclear people that it is possible that the nuclear instruments could have been as much as 10% low during that particular operation.

Estimated Gas Production in the HRE

Earlier in this report it was noted that radiolytic gas production had been predicted to be 11.3 cfm (STP) of $2H_2 + O_2$ per megawatt of reactor power; and the reliability of using heat balance across the recombiners to determine gas production was discussed. During the power operation of the HRE on February 23-24, the following data were taken using the heat balance method.

Estimated Reactor Power kw	Estimated Recombiner Power (Cooling H_2O Balance) kw	cfm (STP) $2H_2 + O_2$ to Produce Heat Removed
70	2.8	0.7
260	9.6	2.4
520	20.8	5.2
540	22.0	5.5
810	31.7	7.9
1000	40.0	10.0

The above data are expressed graphically in Figure 4.

Acknowledgments

This work has been made possible by Messrs. H. M. McLeod, T. S. Mackey, Don Phillips, M. J. Fortenberry, A. D. Ryon, A. A. Palko, and D. W. Kuhn who did most of the early development work; by R. VanWinkle who guided the recombiners through the HRE mock-up stage, and the members of the HRE operating crew and S. E. Beall under whose supervision the recombiners were actually used.

[redacted]
Dwg. 21053

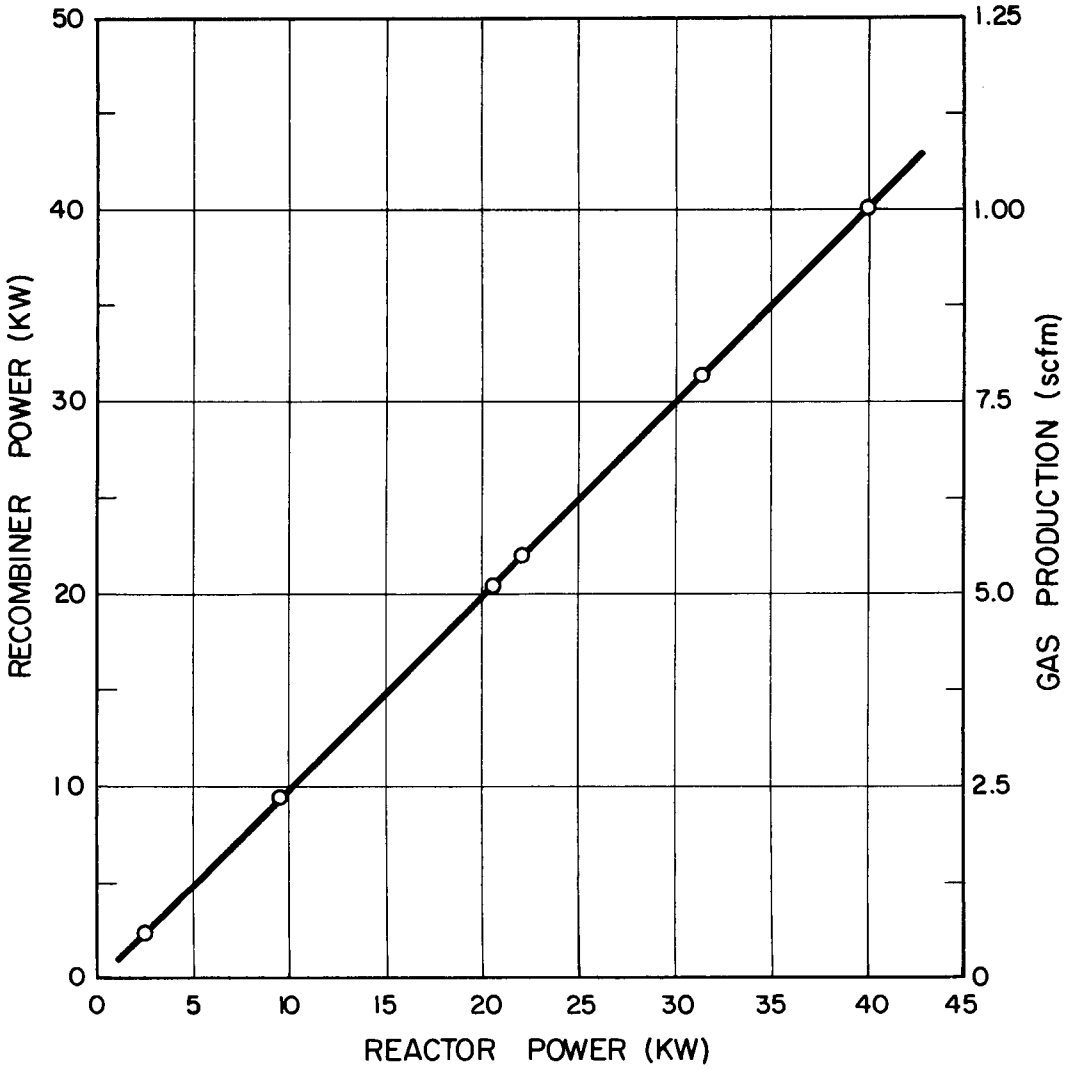

FIGURE 4

GAS PRODUCTION IN THE HRE

CHAPTER II

THE CATALYTIC REACTION OF $2H_2 + O_2$ ON PLATINIZED ALUMINA

Summary

A study is made of the effect of oxygen concentration, temperature from 230 °C to 520 °C, pressure from 25 to 110 psia, and space velocity from 725,000 to 1,850,000 hrs.$^{-1}$. Also, a comparison of the recombination rates of H_2 and D_2 under comparable conditions is made. The reaction controlling mechanism is stated to be diffusion of gas to the catalyst surface, and the basis for this conclusion is developed.

Introduction

In the Intermediate Scale Homogeneous Reactor, it is planned to recombine the radiolytic deuterium and oxygen at reactor pressure, thereby eliminating equipment involved in low-pressure recombination such as a let-down system, a large pulsafeeder, additional heat exchangers, etc. Since the consequences of an explosion starting at a pressure of 1000 psi are likely to be quite severe, and since the only way to guarantee against a deuterium-oxygen explosion is to prevent a combustible mixture from occurring, a flame recombiner of the type used in the HRE is not applicable. The information available on the catalytic recombination of H_2 and O_2 by platinized alumina as of January 1, 1953 was insufficient to enable the design with confidence of a high-pressure catalytic recombiner for the ISHR. Therefore, experiments were planned:

1. To study the effects of excess O_2, flow rate, temperature, and pressure on the reaction rate. The primary range of interest was with excess O_2 present, since this would be the case in the ISHR, for reasons dealing with uranyl sulfate corrosion.

2. To determine if possible the reaction controlling mechanism from the available data.

3. To investigate the applicability of H_2 data for D_2 recombiners.

4. To investigate other catalysts and recombiner types.

5. To investigate the effect of I_2 poisoning quantitatively.

The Apparatus

A simplified flow diagram of the test apparatus is shown in Figure 5. The recombiner consists of a short piece of 1 inch stainless steel pipe with a thermocouple well inserted 1/2 inch into it, and with a steam jacket around it. A 1 1/2 inch section of the pipe is screened off with perforated plates, and the volume within the plates contains 1.39 in.^{3} of 1/8 inch platinized alumina right cylinders. (Figure 6). Steam is admitted to the system through a calibrated orifice, and H_2, or D_2, also metered through a calibrated orifice, is added to the steam. The two gases then flow through a superheater at the base of which a measured quantity of O_2 is added to the mixture. The non-combustible mixture (H_2 concentration varies from 2 to 10 percent, O_2 from 1 to 10 percent) then flows through the catalyst where a portion of the gas is recombined, and out of the system through one or both of two needle valves which control the system pressure. One of the valves is a six-turn, 3/4 inch valve used for coarse control, and the other is a 30 turn, 1/4 inch needle valve, in parallel with the other, used for fine control.

[redacted]
Dwg. 21054

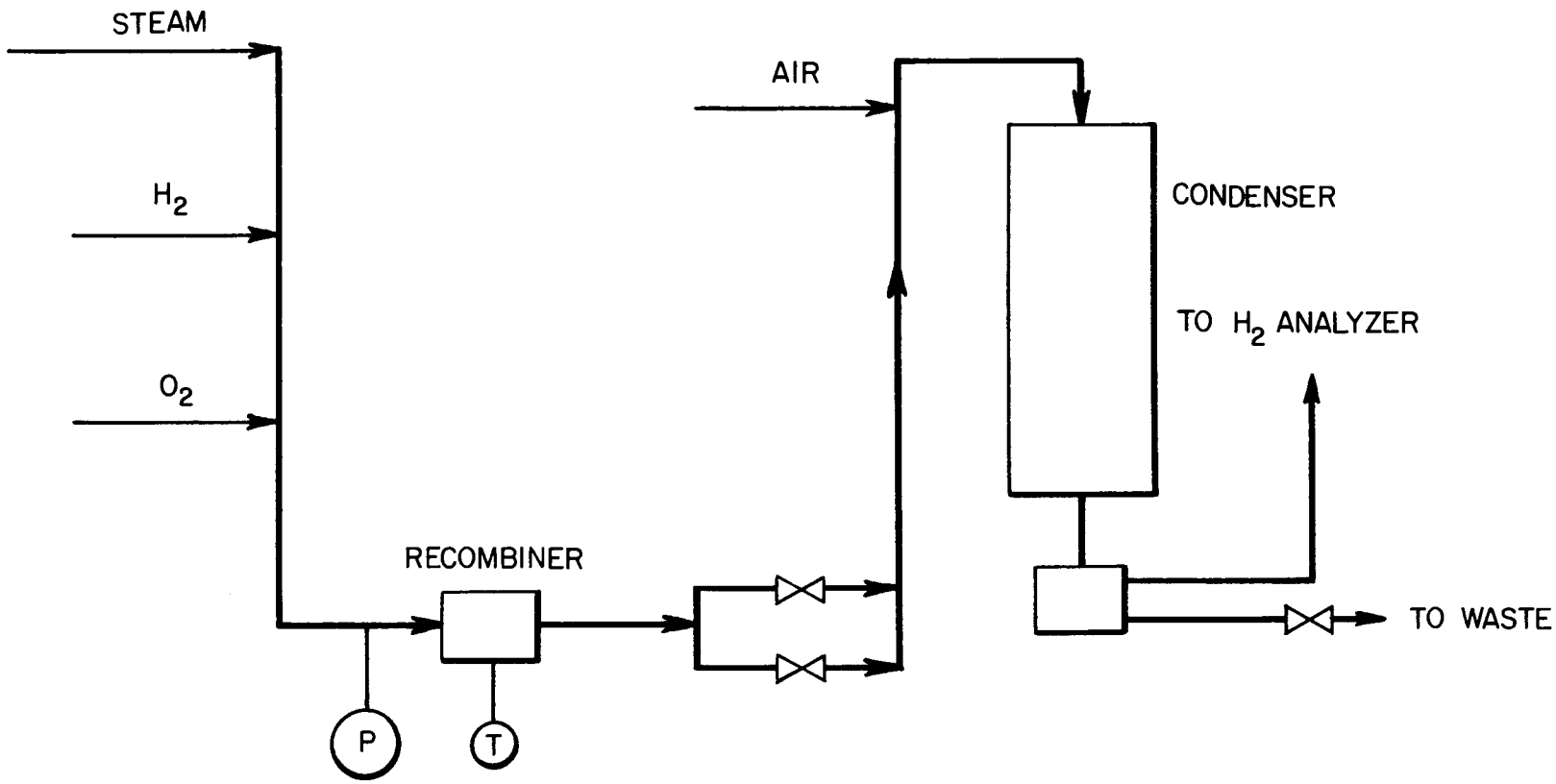

FIGURE 5

TEST CATALYTIC RECOMBINER FLOW DIAGRAM

[redacted]
Dwg. 21055

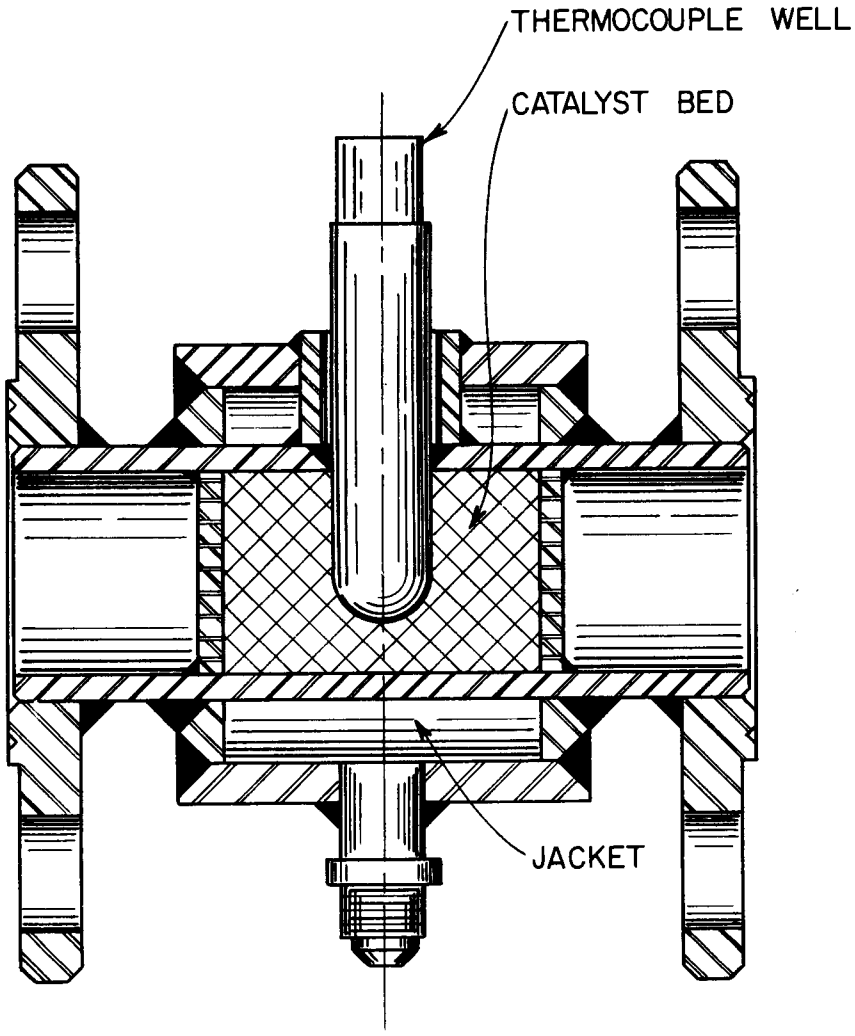

FIGURE 6

CATALYTIC RECOMBINER

After leaving the higher pressure system, the now highly superheated steam-H_2-O_2 mixture is joined by a metered stream of air, and the new mixture then flows through a condenser. At the base of the condenser is a small cylinder in which the condensed water is separated from the air stream. The water and most of the air flow through another pressure controlling valve (condenser pressure is maintained at about 5 psi) to waste. A small portion of the air flows through a drying bed of $CaSO_4$ to a H_2 analyser (see Appendix A). By knowing the amount of air metered into the system and the excess of O_2, and the H_2 concentration of the off-gas stream, one may determine the amount of H_2 which goes through the system unrecombined. The following data were taken for each run: H_2, O_2, steam, and air flow, pressure drop across the recombiner, pressure in the recombiner, temperature in the recombiner, temperature of the gas before and after the recombiner, off-gas H_2 concentration, and various cooling water and other control measurements of no consequence in analysing the recombiner characteristics.

In the interest of safety, the entire high-pressure system from the point where O_2 was admitted to beyond the exit valves was sandbagged, and the valves were remotely operated. The pressure was measured by means of a remote instrument thereby removing the danger of an exploding gage should an accident occur, and rupture discs were located at appropriate places in the system. No accidents occurred.

Discussion of Results

Tests conducted by an MIT Practice School Group* on H_2O-H_2-O_2 mixtures indicated that diffusion of gas to the catalyst surface controlled the reaction rate. As the ratio of O_2/H_2 was increased, the amount of recombination increased, until at ratios above 1, additional O_2 did not increase recombiner effectiveness. This was explained on the basis that at ratios below 1, both hydrogen and oxygen diffusion were important, but above 1 hydrogen diffusion alone controlled the kinetics. Similar results were obtained in the present investigation. Figure 7, which records efficiency vs. O_2/H_2, indicates that the efficiency levels off just above a unit ratio.

[redacted] Dwg.21056

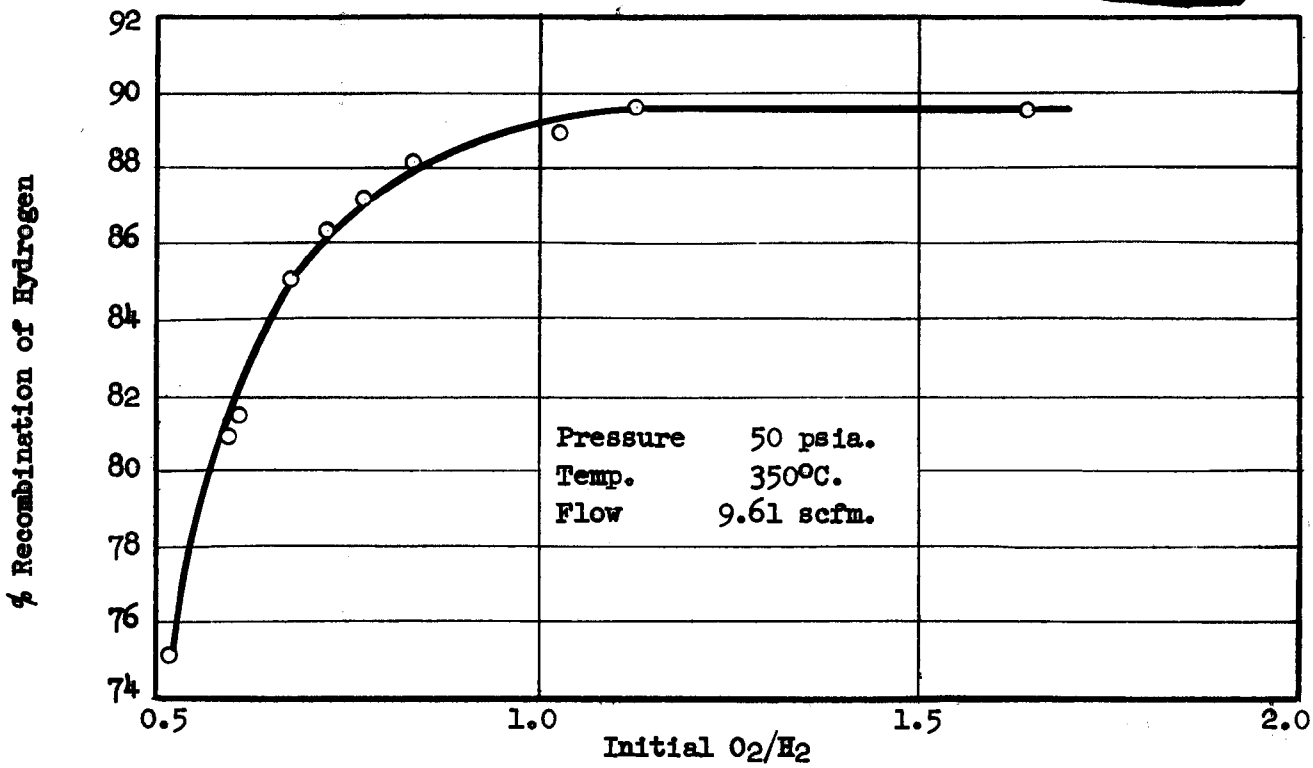

Figure 7

Recombiner Efficiency vs. Oxygen to Hydrogen Ratio

* Gaven, J. V. et.al., "Catalytic Recombination of Hydrogen & Oxygen-II" KT-134 (1952).

For diffusion controlling, three modes of operation exist:

1. Using stoichiometric gas, the diffusion of the heavier component, oxygen, would control rate throughout.

2. With a starting O_2/H_2 greater than 1, hydrogen diffusion would control.

3. With a starting ratio between 0.5 and 1, there would be some point in the bed where the controlling diffusant would change from oxygen to hydrogen.

If diffusion is the only factor governing the reaction rate, the following equation can be derived (Appendix B) to apply to the third mode of operation:

$$\ln \frac{H_f}{2O_o - H_o} = x \ln \frac{O_o}{2O_o - H_o} + \ln \frac{(x-1)^{x-1}}{\left(\frac{x}{2}\right)^x} - \ln f \qquad (1)$$

where H_o is initial hydrogen flow

H_f is unrecombined hydrogen flow

O_o is initial oxygen flow

f is the ratio of H_o/H_f for a run in the same bed at the same temperature, pressure, and total flow rate with hydrogen diffusion controlling throughout.

x is a constant depending on the relative diffusivities of hydrogen and oxygen in steam. $x = \left(\frac{D_H}{D_O}\right)^{2/3}$.

For a given run, values are obtained experimentally for H_o, H_f, and O_o. The quantity f may also be determined experimentally, and was done so during the early development of the method, by operating with enough excess oxygen so that hydrogen diffusion was controlling throughout the bed.

[redacted]

For a series of runs, at constant temperature, pressure and total flow rate, a log-log plot is made of $\frac{O_o}{2O_o-H_o}$ vs. $\frac{H_f}{2O_o-H_o}$. According to equation (1), this should result in a straight line of slope x, with an intercept when $\ln \frac{O_o}{2O_o-H_o}$ is zero of $\frac{(x-1)^{x-1}}{f\left(\frac{x}{2}\right)^x}$. Such a plot for the runs of Figure 7 is shown in Figure 8. The two lowest points have a considerable excess of oxygen, the

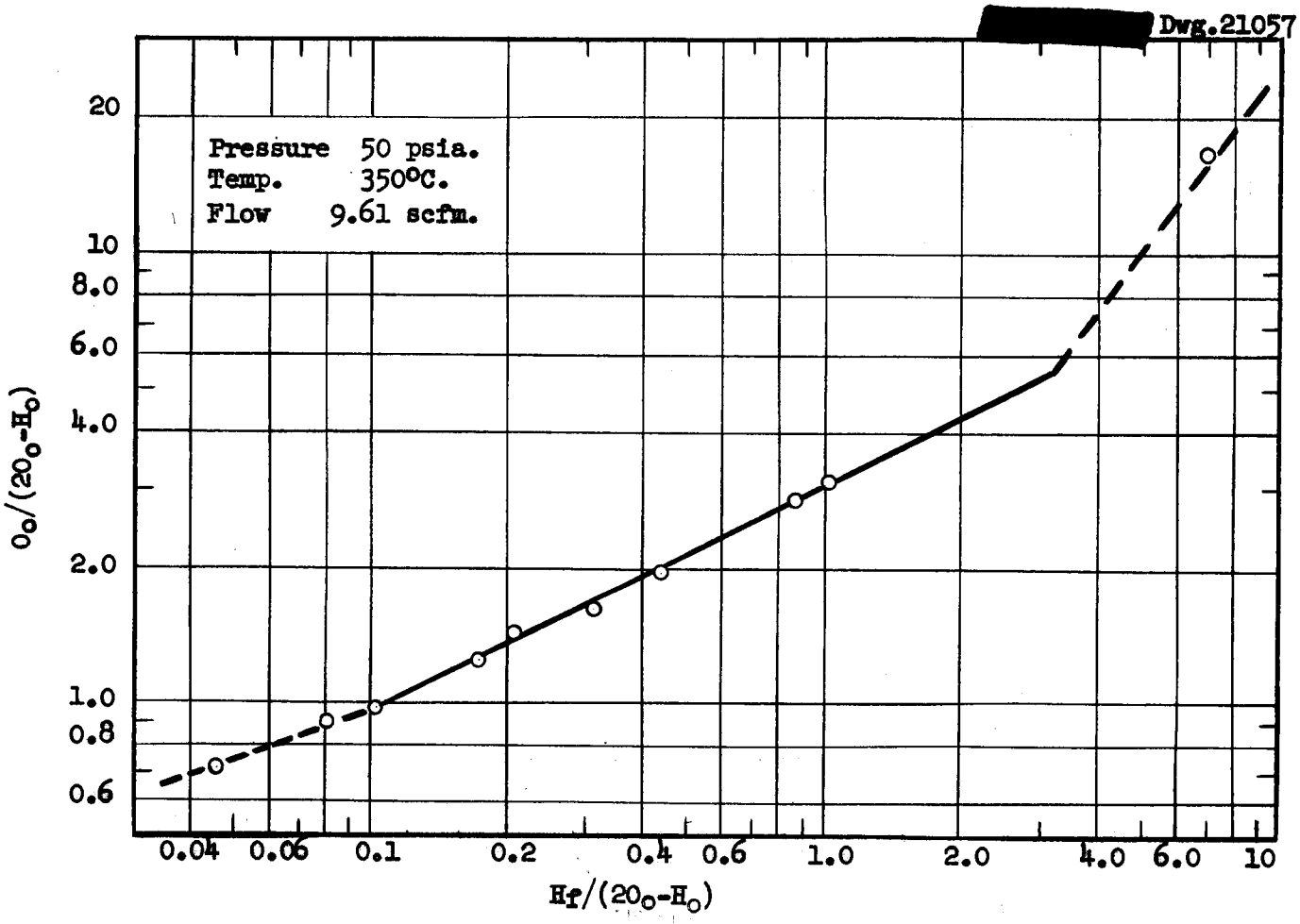

Typical Plot of $\frac{O_o}{2O_o - H_o}$ vs. $\frac{H_f}{2O_o - H_o}$

Figure 8

third point is just on the borderline of hydrogen diffusion controlling throughout, and the uppermost point is in the region where oxygen diffusion controls throughout the bed.

The runs for which equation (1) applies, those in which the diffusion of both components is important, are seen to fall on a straight line whose slope, x, is 2.09. This corresponds to $(D_H/D_O)^{.605}$, based on literature data*. The agreement of the experimental exponent with the theoretical one of 2/3 is believed to be excellent, since there is considerable uncertainty in the diffusivity data and also in the theoretical exponent.

The intercept of Figure 8 indicates that f equals 9.1. The value of f obtained experimentally from the lowest three runs shown varies from 9.1 to 9.7.

Another observation may be made from the slope of Figure 8. The O_2/H_2 ratio at which the recombination levels off should be x/2, the ratio which is shown in Appendix B to be the demarcation between oxygen and hydrogen controlling. The value of x/2 from Figure 8 is 1.05; in Figure 7, the recombination levels off just above 1.

---

* The hydrogen-steam diffusivity is listed in the International Critical Tables. The oxygen-steam diffusivity was obtained by a minor correction on the air-steam diffusivity of ICT, using the Gilliland equation. The theoretical 2/3 exponent is based on the Chilton-Colburn mass transfer correlation. Both Gilliland equation and Chilton-Colburn correlation are found in Hougen and Watson, "Chemical Process Principles", Vol. 3, Chapter XX, John Wiley & Sons, New York (1947).

The consistency with which the experimental data fit the correlation strenghtens the contention that the recombination is diffusion-controlled.

Figures 9-12 are plots of $\frac{O_o}{2O_o-H_o}$ vs. $\frac{H_f}{2O_o-H_o}$ at temperatures ranging from 231 to 515°C. and pressures of 30 to 110 psia. The flow rate was maintained close to 13.2 standard cfm. The slopes of all the lines are close to 2.1.

The variation of reaction rate with temperature and pressure can best be seen in Figure 13, which is a graph of mass transfer coefficients with temperature and pressure parameters. The coefficients, which are hydrogen-controlling, are calculated from the plots of Figures 9-12 by means of the following equation:

$$M(h_o-h_f) = K_H\ A\ \Delta\ h_{lm} \qquad (2)$$

which simplifies to:

$$K_H = \frac{M \ln (h_o/h_f)}{A} = \frac{M \ln f}{A} \qquad (3)$$

where:

M is total mol flow rate, lb. mol/sec.

h_o and h_f are initial and final hydrogen mol fractions

K_H is hydrogen mass transfer coefficient $\frac{\text{lb. mol.}}{\text{sec.ft.}^2\text{(mol. fraction)}}$

A is total area of catalyst pellets, ft.^{2}

Δh_{lm} is log mean mol fraction driving force with hydrogen concentration at catalyst surface being zero.

f is h_o/h_f defined previously under equation (1).

[redacted]

Dwg. 21058

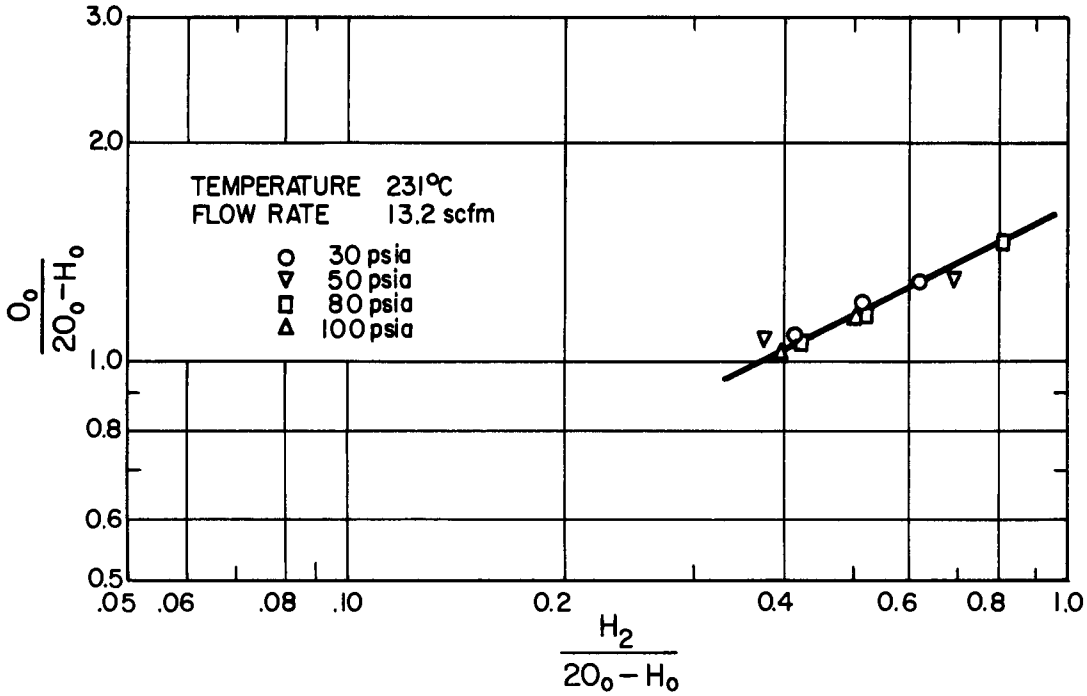

FIGURE 9

PLOT OF $\frac{O_o}{2O_o - H_o}$ VS $\frac{H_f}{2O_o - H_o}$ AT 231°C

[redacted]

Dwg. 21059

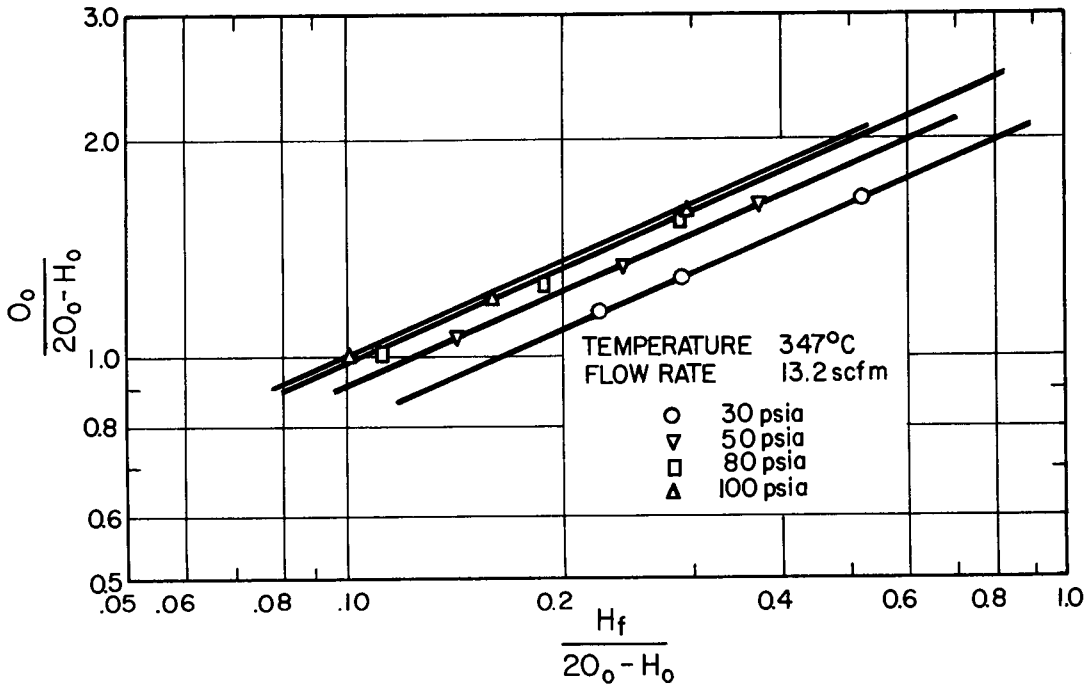

FIGURE 10

PLOT OF $\frac{O_o}{2O_o - H_o}$ VS $\frac{H_f}{2O_o - H_o}$ AT 437°C

[redacted]

Dwg. 21060

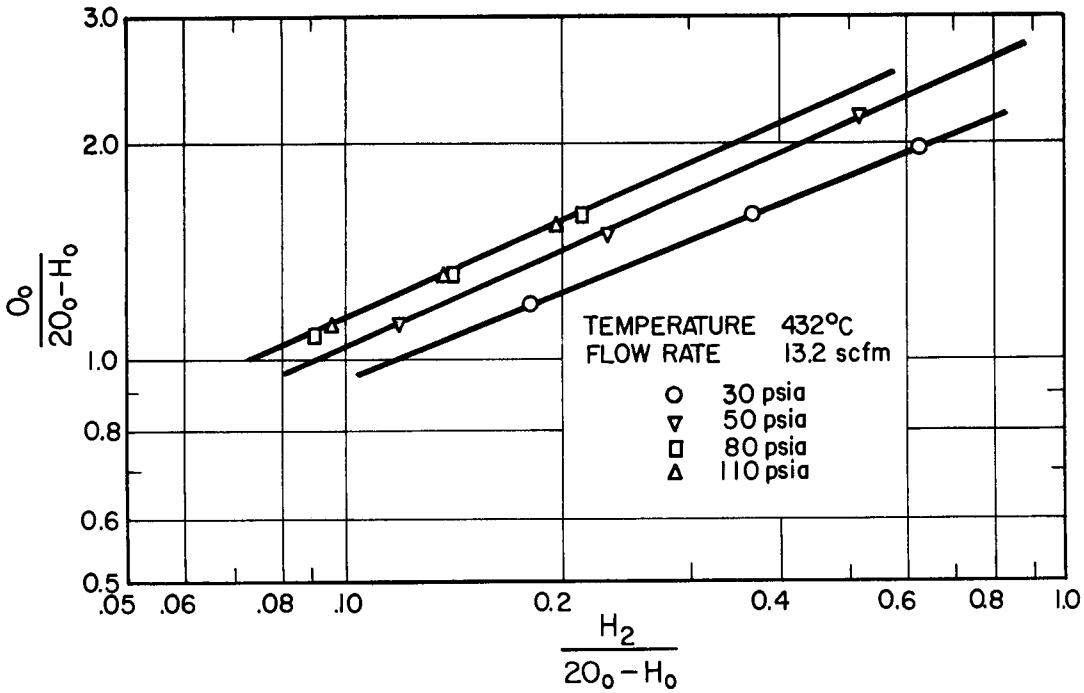

FIGURE 11

PLOT OF $\frac{O_o}{2O_o - H_o}$ VS $\frac{H_f}{2O_o - H_o}$ AT 432°C

[redacted]

Dwg. 21061

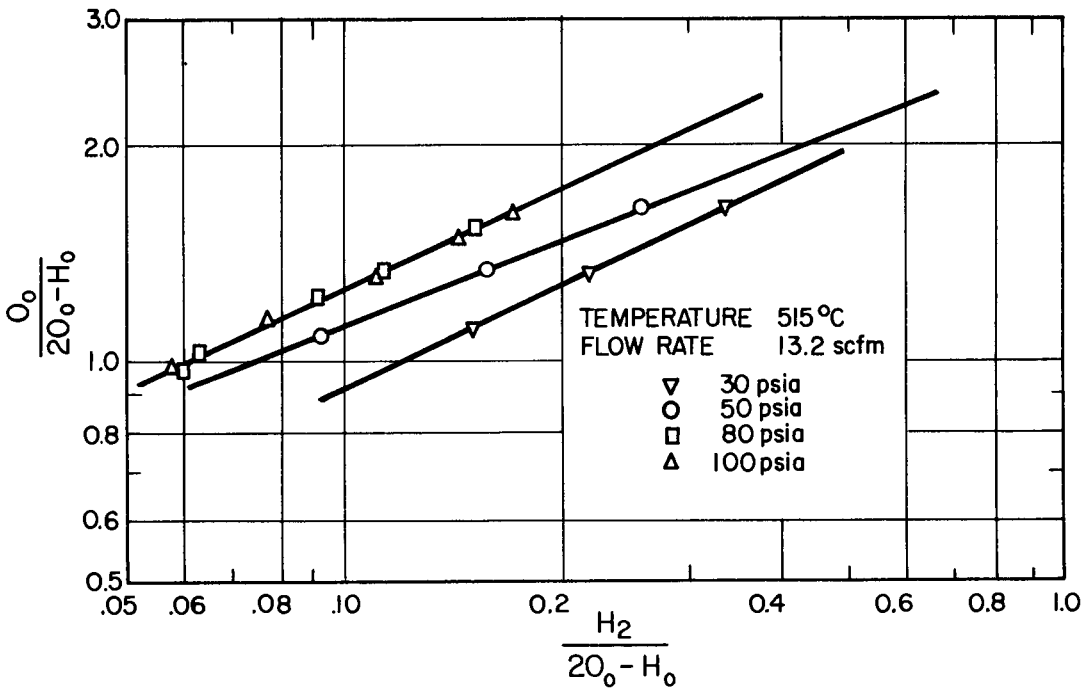

FIGURE 12

PLOT OF $\frac{O_o}{2O_o - H_o}$ VS $\frac{H_f}{2O_o - H_o}$ AT 515°C

It can be seen that the mass transfer coefficients (recombination rates) increase gradually as the temperature is increased, at temperatures above 300 °C. The kinetics at 231°C appear to be abnormally low, indicating probably that the chemical and adsorption kinetics on the catalyst surface are coming into play. The theoretical coefficients (Appendix C) are also plotted in Figure 13, and they increase slowly with temperature.

The effect of pressure on recombiner efficiency appears to be that increasing pressure aids recombination, particularly close to atmospheric pressure. At 100 psia. the effect of pressure change appears to be much less; perhaps the mass transfer coefficients are approaching an asymptotic value. Diffusion theory predicts a mass transfer coefficient independent of pressure. The experimental dependence may be explained by postulating multimolecular layers of the non-controlling diffusant adsorbed on the platinum surface, through which the controlling diffusant must travel. Since the resistance of such a layer might change very little with pressure, the relative resistance of the layer and the true gas film might be negligible at high pressures, but appreciable at the pressures of the current investigation.

Figure 14 shows the change in hydrogen mass transfer coefficients with flow rate, at constant temperature and with a pressure parameter. The curves are parallel to the theoretical diffusion-controlling curve, but they lie about a factor of three below the theoretical. It is believed that channeling can account for the discrepancy.

[redacted]
Dwg. 21062

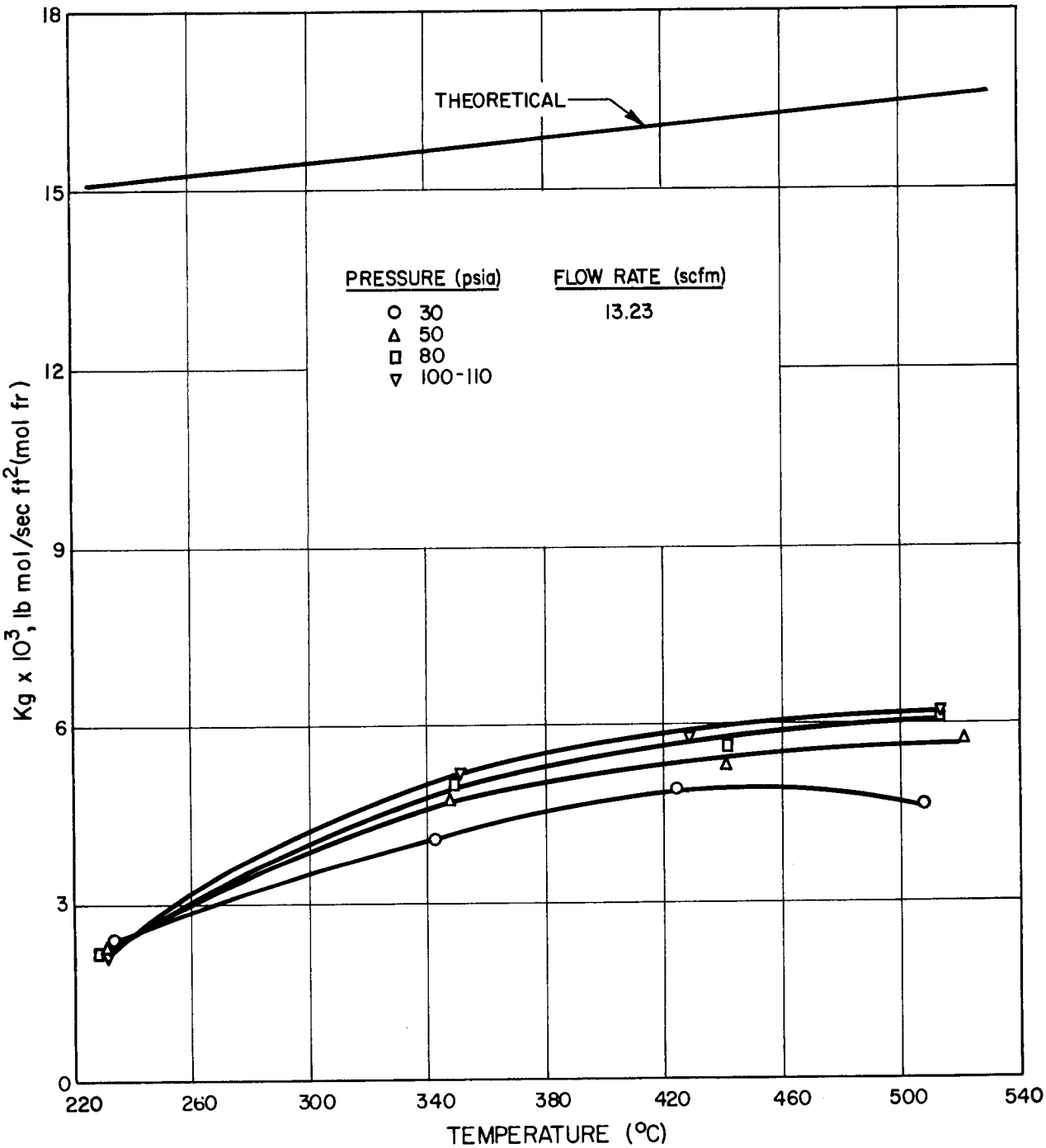

FIGURE 13

HYDROGEN MASS TRANSFER COEFFICIENTS AS A FUNCTION OF TEMPERATURE AND PRESSURE

[redacted]

Dwg. 21063

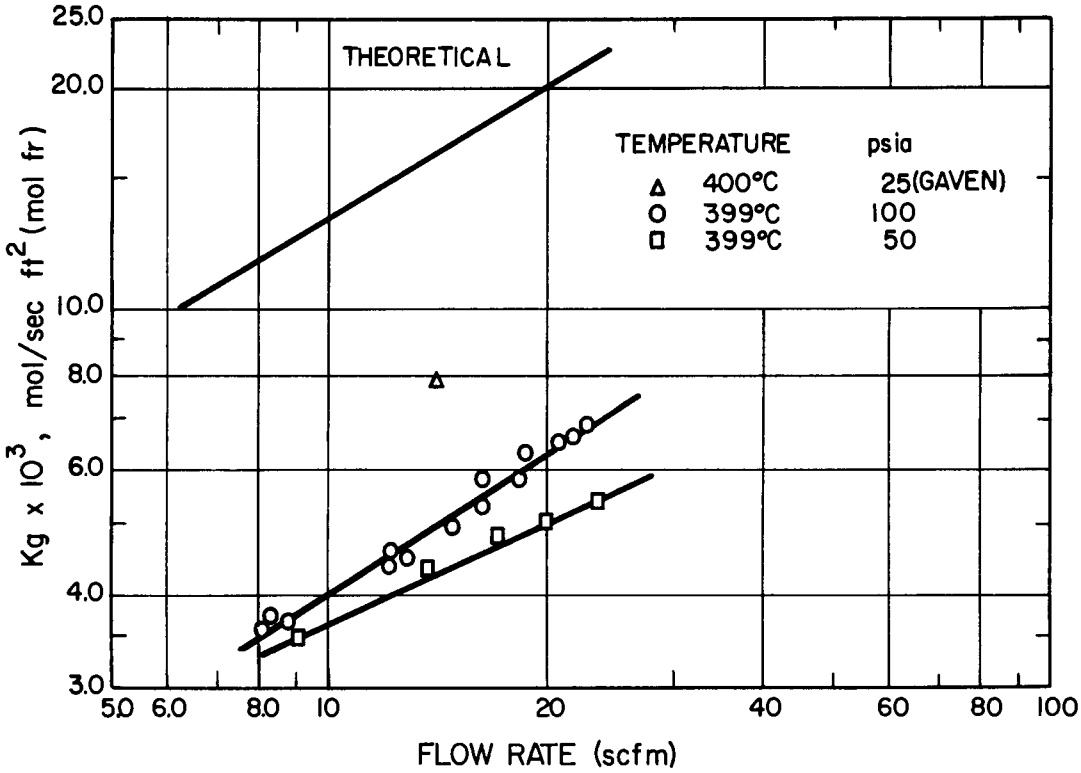

FIGURE 14

HYDROGEN MASS TRANSFER COEFFICIENTS AS A FUNCTION OF FLOW RATE

Normal channeling in a bed of granular particles where the particle diameter is 1/8 the bed diameter causes a decrease in the friction factor of 0.67*. Since the friction factor is proportional to the mass transfer coefficient, according to the heat transfer-mass transfer-momentum transfer analogy, the same change would occur in the mass transfer coefficient. The test bed was further handicapped by a large thermocouple well, and entrance and exit distributor plates with a small amount of hole area.

A better bed, also in a 1-in. pipe, but with no thermocouple well, was tested by Gaven, et. al.** This bed contained an entrance screen of high porosity and no exit screen. The major portion of their investigation was in the oxygen-diffusion controlling range, but one point in the hydrogen-controlling range, based on the average of three runs, is plotted on Figure 14. Although the Gaven point is at lower pressure than the curves of the present investigation, the mass transfer coefficient is about twice as high. Combining the probable effects of normal channeling and abnormal channeling introduced by poor bed design, the experimental results of the present investigation are brought quite close to the theoretical mass transfer predictions.

---

* Perry, "Chemical Engineers' Handbook", 3rd edition, p. 394, (1950)

** Gaven, et. al., op.cit.

In order to evaluate the relative recombination rates of deuterium and hydrogen, a series of carefully controlled runs were carried out at 350°C. and 50 psia. varying the amount of excess oxygen. These are plotted in the usual manner in Figure 15. The deuterium line is seen to fall below the hydrogen line, which is expected because of its lower diffusivity. However, the slope of the D_2 line, which remains 2.1, according to the theory developed previously should have decreased to about 1.74.

Its failure to conform to the predicted slope may be caused by the catalytic exchange reaction, $D_2 + H_2O = HD + HDO = H_2 + D_2O$, which occurs quite rapidly on a platinum catalyst. This side reaction should have been quite important in the oxygen-diffusion-controlling range, where an adsorbed D_2 would find an H_2O molecule much quicker than an O_2. It is believed that in a heavily oxidizing region, such as the platinum surface in the deuterium controlling range, the exchange reaction was retarded considerably. Nothing quantitative can be gained from this speculation; apparently the D_2 runs should have been carried out with a D_2O diluent rather than the normal steam.

It is possible to calculate a deuterium mass transfer coefficient for the run shown in the lowest point of Figure 15, which was deuterium-controlled for the entire bed. The table below compares the predicted and observed mass transfer coefficients for deuterium and hydrogen. An oxygen mass transfer coefficient, obtained in the same series of hydrogen runs, is also listed.

[redacted]

Dwg. 21064

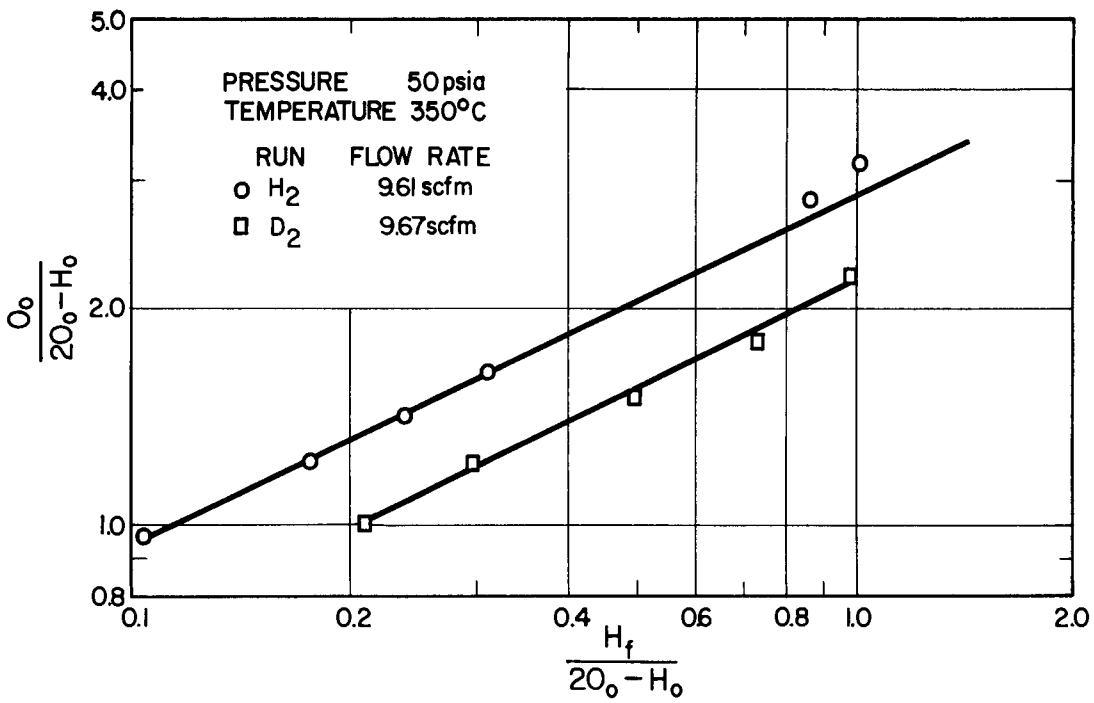

FIGURE 15

COMPARISON OF HYDROGEN AND DEUTERIUM DATA

Mass Transfer Coefficients, Lb. Mol/Sec. Ft.^{2} (mol fraction)
Temperature-350°C.- Pressure-50 psia.- Flow Rate- 9.65 scfm.

Diffusant	Observed Coefficient	Predicted Coefficient	Observed / Predicted
Hydrogen	3.52×10^{-3}	13.05×10^{-3}	0.270
Deuterium	2.58×10^{-3}	10.72×10^{-3}	0.240
Oxygen	2.05×10^{-3}	5.78×10^{-3}	0.355

Based on the hydrogen diffusion, the deuterium diffusion was somewhat poorer than expected and the oxygen diffusion somewhat better.

Reliability and Possible Sources of Error

The possible sources of error in this work lie predominantly in the flow measuring devices. One major exception to that generalization is the seriousness of a leak of any kind in the high pressure system. Early in the experimentation a leak did develop, but it was stopped, and great pains were taken to see that no others developed. There are several concrete check points which do testify to the lack of a leak in the system during the operations which led to the data reported herein. First, the presence of a leak would cause the apparent effect of pressure on recombination to increase with increasing pressure rather than decrease as was the case. Also, pressure control, recombiner temperatures and variations in pressure drop through the bed were of such consistency as to give confidence in the tightness of the system.

The H_2 analyser was found to be sensitive to very small changes in H_2 concentration, and the air metering system which measured the diluent air into the system was found to be reliable. Furthermore, the H_2 analyser was recalibrated a few times each day, and no drift was discovered, testifying to the validity of H_2 off-gas measurements.

The H_2, O_2 and air meters were all calibrated by a wet test meter, and are believed to be accurate within 2 or 3 percent. The steam orifice was calibrated by weighing condensate, and it is believed that an error of several percent is possible in the steam measurements. Furthermore, the steam measuring system has been known to accumulate some condensate, and this condition caused occasional errors in measurement. In fact, the space velocities for two of the points (they are asterisked in Appendix E) in the flow rate data were calculated from the recombiner temperature and the H_2-O_2 flow because the steam flow measured was in doubt and unreasonable, and pressure drop data also lent support to the calculated rather than the directly measured values for steam flow.

The pressure measuring device had a drift of several psi. throughout a day's operations, but showed no permanent drift.

Conclusions

1. It is concluded that diffusion of hydrogen and oxygen to the catalyst surface is the controlling resistance to the recombination. The design of an actual bed operating at temperatures above 300°C. may be calculated on the basis of the usual Chilton-Colburn correlation for mass transfer. Care should be taken that channeling is minimized; if this is done then a safety factor of 2 in the thickness of the bed is considered very conservative for all operating pressures.

2. For temperatures below 300°C., chemical and adsorptive rates enter into the picture. The safety factors for bed design should be increased in a manner consistent with the data of this investigation. For temperatures below 230°C., for which no quantitative data are available, additional experimental work is required to permit good design.

3. The difference in the recombination rates of deuterium and hydrogen is attributed to the difference in the diffusivities. The chemical and adsorptive activity of the two appear to be comparable for the catalytic recombination.

4. Because of the lack of experimental information, no conclusions as yet are made on the effect of fission product poisons, or the life of the catalyst. In the two months of intermittent operation, no deterioration of the catalyst was observed, although there was an accumulation of rust.

Future Plans and Recommendations

1. It is planned to operate a high pressure recombiner loop. The objectives of this system are to investigate the life of the catalyst and the structural materials at ISHR design pressure and temperature, and to confirm the tentative recombiner design based on the diffusion-controlling mechanism. The relative severity of explosions at varying deuterium (or hydrogen) to oxygen ratios will be evaluated.

2. It is planned to evaluate experimentally the amount of iodine poisoning likely to occur in the ISHR system.

3. It is planned to operate a small-scale system simulating the ISHR, to test the relation between the various components involved in the gas system. Startup procedures will be defined.

4. For other investigators of the H_2-O_2-H_2O catalytic recombination, it is suggested that additional information on the reaction should be obtained in the hydrogen-rich region. This was not done here because it is outside the ISHR specifications.

CHAPTER III

THE DEVELOPMENT OF AN EXPLOSION PROOF, AUTOMATIC LOAD ADJUSTING, FLAME RECOMBINER

Summary

The advantages, possible uses, and operating characteristics of a new type, safer, lower temperature flame recombiner are described. It is particularly adaptable to reactors where the radiolytic gases that are evolved are associated with large quantities of steam such as in a boiling reactor. Due to a lack of time, the information reported here is mostly qualitative, but the method definitely has been proven valid.

Introduction

McLeod et al*, found that H_2-O_2-steam mixtures containing less than 25 percent $2H_2 + O_2$ in a pipe would arrest the explosion of a combustible mixture of the gases elsewhere in the system. In a boiling reactor, the radiolytic gases produced are expected to be only about 1 percent of the steam volume concurrently evolved. The total volume depends upon the power level of the reactor. It was reasoned that as the steam-gas mixture travelled up the condenser which is used to remove power from the system, the mixture would eventually lose enough steam to become combustible. The location of the first combustible gas would depend upon the power level of the reactor. It follows then, that if one could distribute ignition sources

---

* H. M. McLeod et al, Recombination of Stoichiometric Mixtures of H_2 and O_2 in a Flame Recombiner (Feasibility Report), ORNL, Y-706, 1951. [redacted]

(for example spark plugs) throughout the condenser, wherever the gas became combustible it would burn, and the noncombustible front directly behind the flame would protect against flashbacks. In order to test the validity of this idea, a column containing alternating cooling coils, and spark plugs was constructed, and means were provided to add steam, H_2 and O_2 to the column, and to remove water from the bottom and unrecombined gas from the top.

The Apparatus

A drawing of the apparatus is shown schematically in Figure 16, and a detail of a section is shown in Figure 17. The cooling coils, of course, serve to condense out part of the steam admitted, the spark plugs to provide an ignition source, the thermocouples to indicate the temperature at various points in the system, and the sight glasses to allow visual observation of the combustion. A 3-inch thick plexiglass shield was placed directly in front of the apparatus to protect operators in the event of an accident, of which there were none.

The steam, H_2, and O_2 were metered into the system through calibrated orifices - the same ones described in Section II of this report. Pressure was controlled by adjusting the O_2 excess and the opening of the remotely operated valve, at the upper outlet of the column, and the condensed water was allowed to flow through a valve at the base of the column, the valve operation being controlled by a differential pressure cell which was activated by the water level in the column.

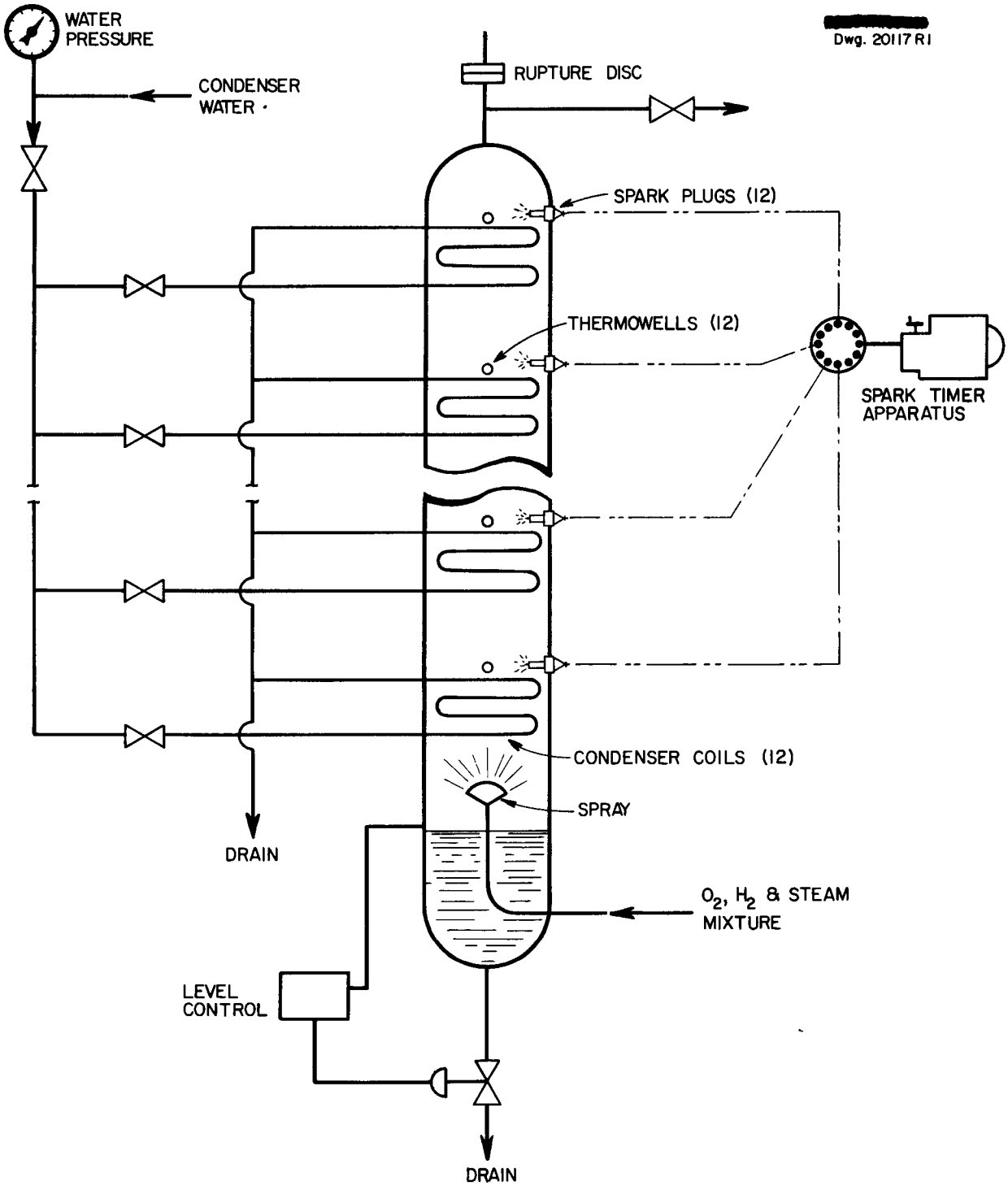

FIGURE 16

EXPERIMENTAL FLAME RECOMBINER FLOWSHEET

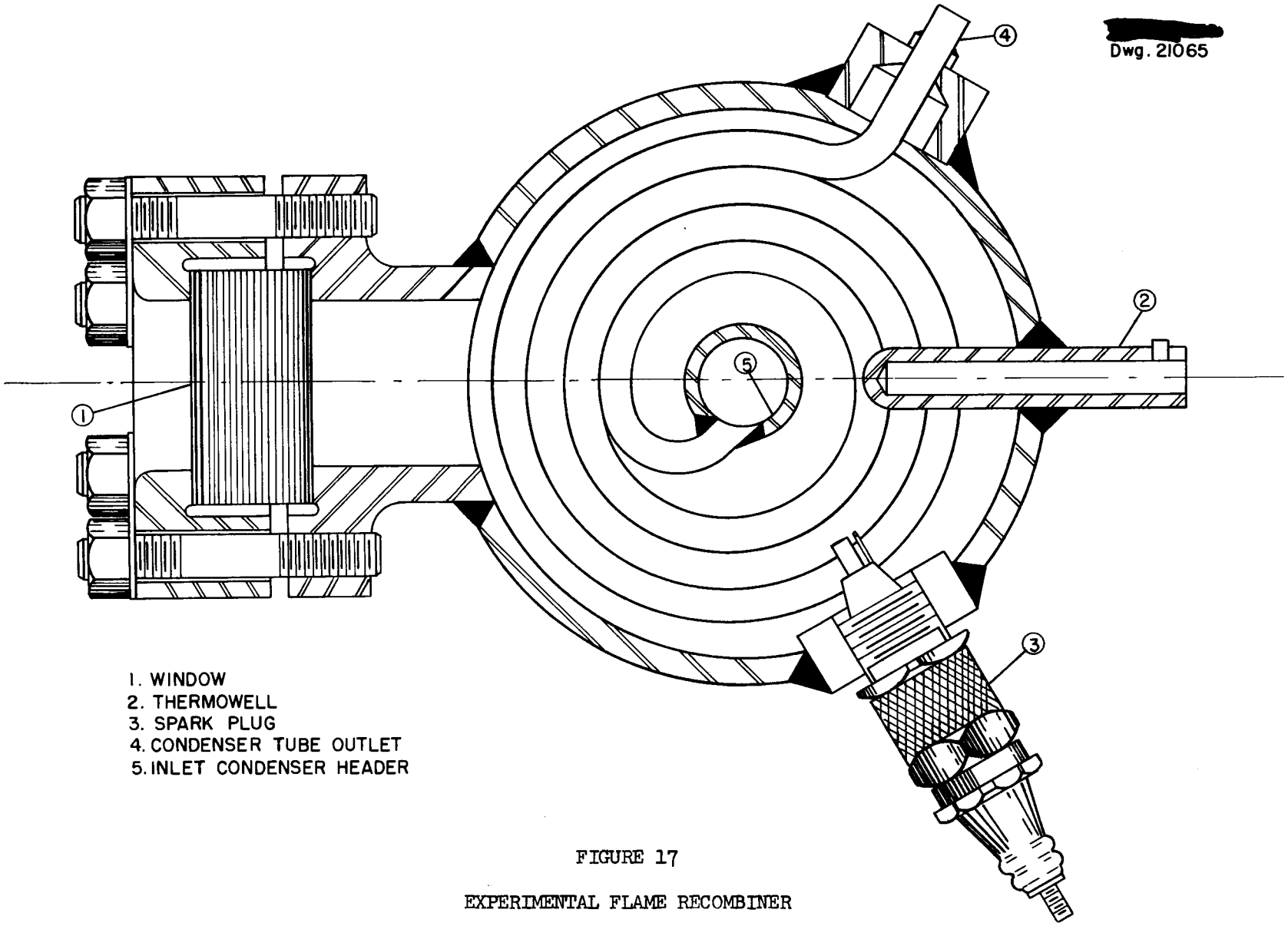

1. WINDOW
2. THERMOWELL
3. SPARK PLUG
4. CONDENSER TUBE OUTLET
5. INLET CONDENSER HEADER

FIGURE 17

EXPERIMENTAL FLAME RECOMBINER

The H_2 analyser described in the previous section was also used in this work. Diluent air was admitted downstream from the pressure control valve.

The spark impulse was generated by an automobile battery charger, connected in series with an induction coil; the spark was distributed to the 12 plugs by a Lincoln distributer driven by an electric motor. The spark gap was adjusted to 1/8 inch. The plugs were protected from shorts, due to water dripping on them from the condenser coils above, by a sheet metal shield located just above the spark gap.

Operating Characteristics

Noncombustible mixtures of H_2, O_2 and steam (usually containing about 5 to 15 percent H_2) were admitted to the bottom of the column described in the previous section. The column's temperature profile could be directly attributed to the partial pressure of steam at the position of the thermocouples in the column from the bottom thermocouple up to thermocouple No. 6 (the thermocouples are numbered from the top). That is, the bottom two or three were at the same temperature, that being the boiling point of steam at column pressure; and the next few points were somewhat lower due to the reduced partial pressure of steam in the system.

However, thermocouple No. 6 began to rise sharply upon the introduction of H_2 to the system, as did the thermocouples No. 5 and No. 4, immediately above it. Gas flow, which at first was less than one cfm (STP) of $2H_2 + O_2$ (plus a slight excess of O_2), was then gradually increased until the flow of H_2 and O_2 reached 9.6 cfm. At no point during the transition from less than one to 9.6 cfm of

$2H_2 + O_2$ flow were any pressure surges or other types of instability noticed in the system. Furthermore, once the flow reached 3 cfm, the maximum temperature appeared to have been reached in the system.

With a flow of 3 cfm of $2H_2 + O_2$, a temperature of 320°C was noted at thermocouple No. 6, the temperatures below that corresponding to partial pressures of steam as described earlier, and the temperatures of the thermocouples above ranging from a little above 200° down to about 50°C. As the flow was increased, the temperature at No. 6 was seen to remain essentially constant, and the temperatures of thermocouples 1 through 5 rose considerably until they were all above 150°C.

All during this period, the column was being operated with a slight excess of O_2. The column pressure was maintained at approximately 60 psi by throttling the outlet valve at the top of the column. The H_2 analyser indicated a recombiner efficiency of 99.5 to 99.98 percent, depending upon the amount of excess O_2 used. It was decided that if stoichiometric gas could be admitted to the system, and the valve at the top completely closed off, it might be possible to obtain recombiner efficiencies of 100 percent.

This was done, with the capacity remaining about the same. It was, of course, impossible to obtain exactly stoichiometric mixtures of H_2 and O_2, so the column was operated between 50 and 70 psia pressure, the pressure rising when an excess of O_2 was being admitted, and falling when H_2 flow was increased. This somewhat questionable procedure proved to be satisfactory over relatively short periods of operation, but would doubtlessly become quite trying if the period of operation were to be increased to several hours.

During the total recombination operation, it was noticed that thermocouple No. 1, the one at the top of the column eventually became hottest -- 350°C. This may be explained by recalling that during open operation of the column, the amount of unrecombined H_2 increased with increased excess O_2. Apparently, combustion of the gases in the presence of a diluent is incomplete. At high flows of combustible gas, the H_2 concentration in the noncombustible residue at the top of the column increases quite rapidly, and as a result there is enough combustion at the No. 1 spark plug to maintain a relatively high temperature in that region. A sample curve of gas flow vs. thermocouple temperature is shown in Figure 18. This curve is not exactly reproducible due to inability to exactly duplicate conditions.

At no time during the operation of this machine was a visible flame established at any point; and the operation was completely free of flashbacks. There were occasions when burning was observed in "noncombustible" regions, but this may be explained as being due to channelling effects, and such combustion was definitely not extensive. The dependence of the column on a noncombustible front for smooth operation was displayed as the result of an accident during one period of operation. The valve at the base of the column failed to operate properly, and a sizeable leg of water built up in the column; the bottom six condensing coils were covered. The result was that the column of water was cooled by the cooling water circulating through the coils, and steam was in turn removed from the gas bubbling through the column of water present in the bottom of the column. No longer were small amounts of gas being burned while the whole mixture was still noncombustible, and no longer

[redacted]
Dwg. 21066

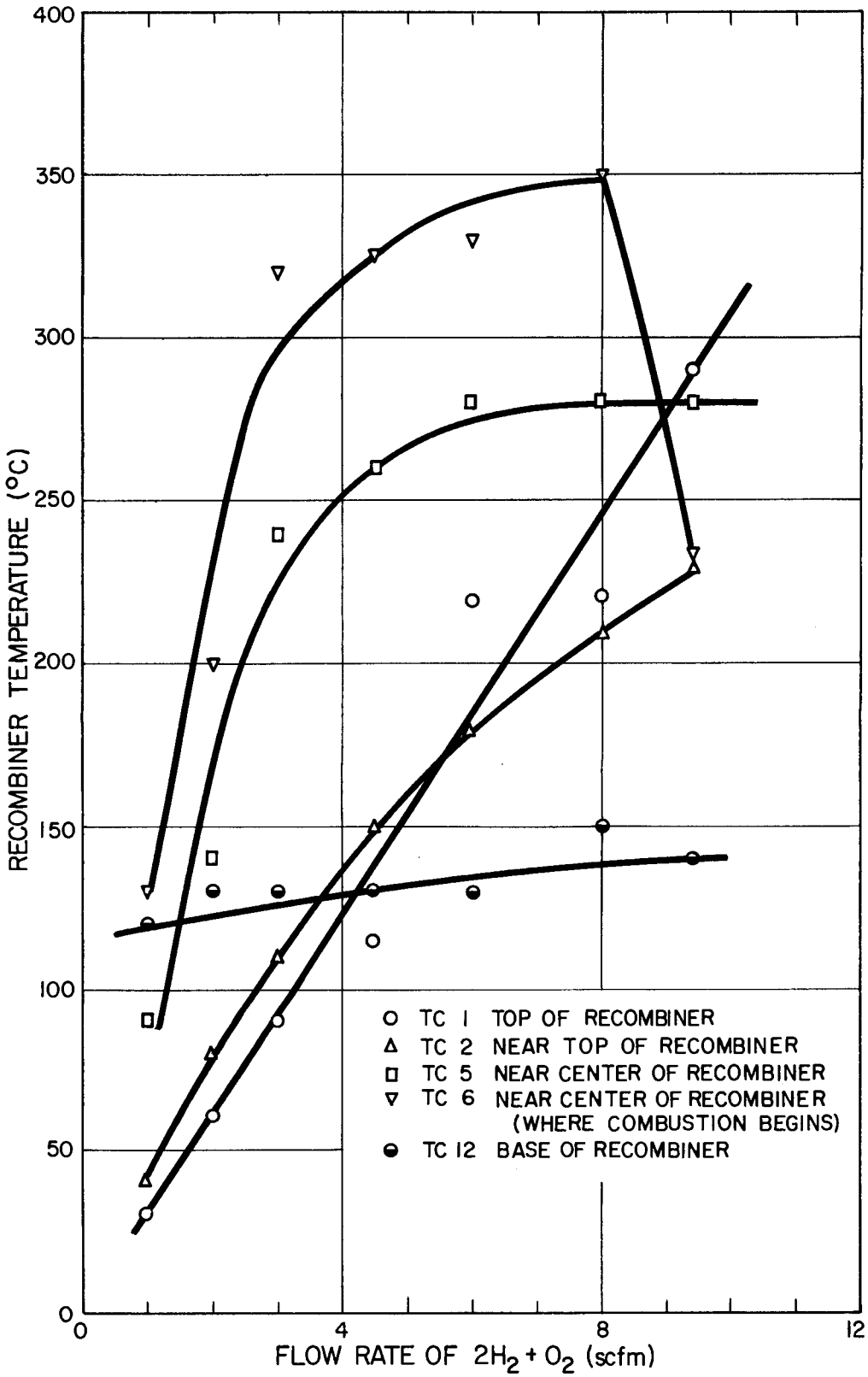

FIGURE 18

FLAME RECOMBINER TEMPERATURE VS. GAS FLOW RATE

were there spark plugs every few inches which could ignite the gas as soon as the mixture became combustible. Instead, the gas leaving the water leg was highly combustible, and a series of explosions ensued.

The gas flow was left on while attempts were made to reopen the valve at the column's base, and meanwhile the explosions continued and became worse. The explosions were not only evidenced by mild pressure surges, (mild due to the slowness of the pressure instrument) but persistant orange-red flashes could be seen through the sight glasses as well. When it became obvious that the valve trouble would not be quickly remedied, and that as the column of water continued to rise the explosions would become more violent, the apparatus was shut down.

Conclusions

This type of recombiner will certainly operate satisfactorily and is definitely applicable to boiling reactors in general and the proposed "teapot" in particular. Additional and more quantitative testing is necessary, and certainly a combustion apparatus of this type must be tested at high pressures before being used in a reactor. However, its usefulness and applicability have been demonstrated by this work. It will probably be necessary to use some other type of ignition source in higher pressure work, but this is not an insurmountable problem.

Acknowledgments

To Robert Cauble, Paul R. Kasten, R. N. Lyon, E. R. Baxter, Royce Goodman, W. B. Pike, Cecil Hubbard, Harold Gutherie, W. P. Walker, and J. R. McWherter for able and enthusiastic assistance.

/gd

APPENDIX A

A Catalytic Combustion Hydrogen Gas Analyser

Description of the H_2 Analyser

The analyser consists of two sensing cells and a cell block as shown in Figure 19. The first cell is an active element with an electrically heated platinum wire, while the second cell is a reference element of alumel wire also electrically heated.

Each of the elements, which are in series in the gas stream, has a thermocouple spot welded to the center of the heater wire. The heaters are 10 mil diameter wire and the thermocouples are made from 12 mil chromel-P and 10 mil nickel wires. The aluminum cell block is 4 1/2 x 2 x 2 inches and the sensing cells are 1 1/4 x 1 x 1 1/2 inches over-all.

Operation

Figure 20 is a schematic diagram of the complete analyser system. A sample stream is taken from the process line, dried by passage through a calcium sulphate bed, and then introduced into the cell block. A constant differential pressure relay and needle valve are used to hold the flow through the cells at approximately 0.6 CFH.

Figure 21 is a schematic drawing of the heater current control and thermocouple circuit. To place the analyser in operation, the platinum wire current is adjusted to approximately 3 amperes and then the alumel wire current is

UNCLASSIFIED
Dwg. 21067

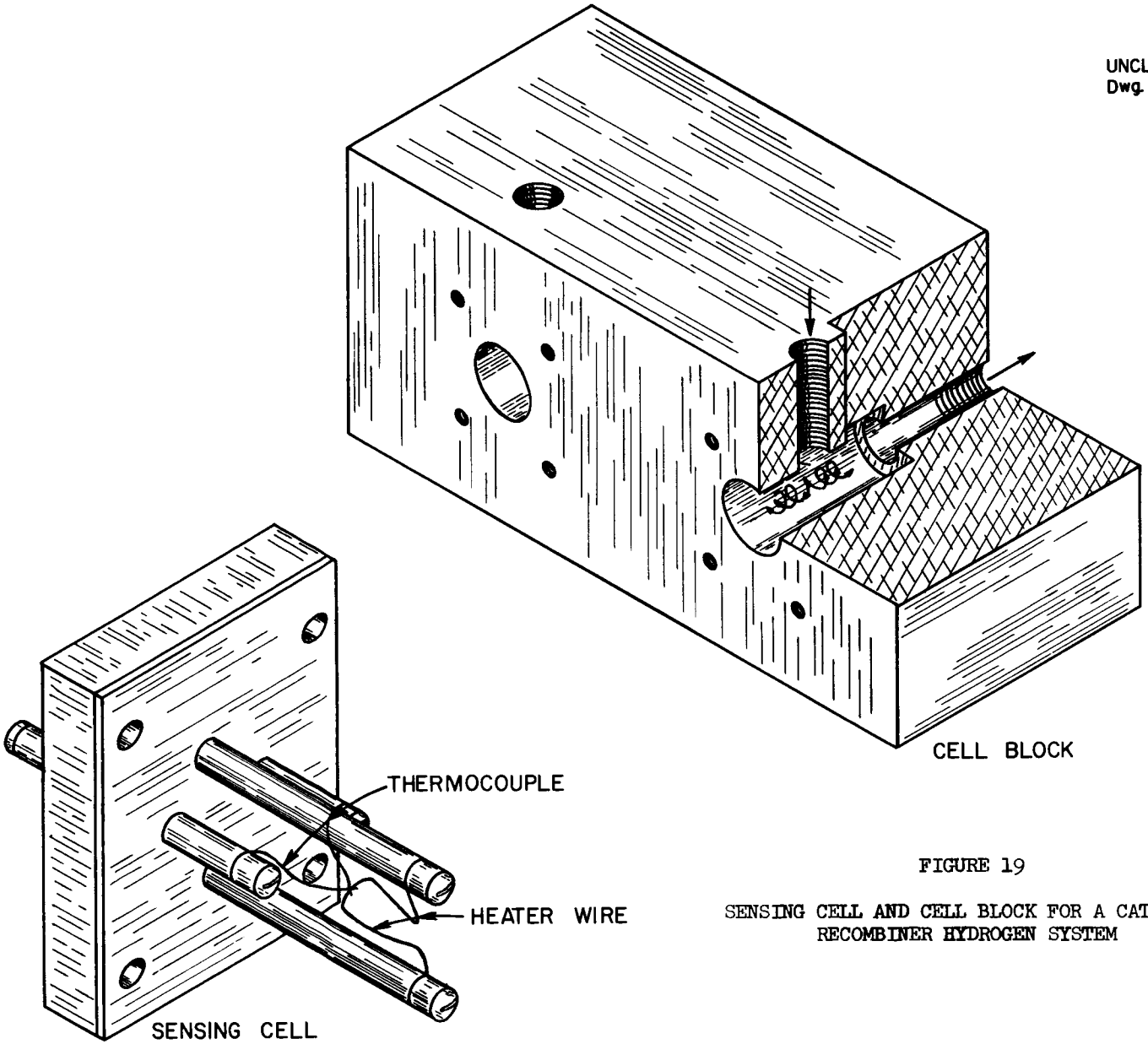

FIGURE 19

SENSING CELL AND CELL BLOCK FOR A CATALYTIC RECOMBINER HYDROGEN SYSTEM

UNCLASSIFIED
Dwg. 21068

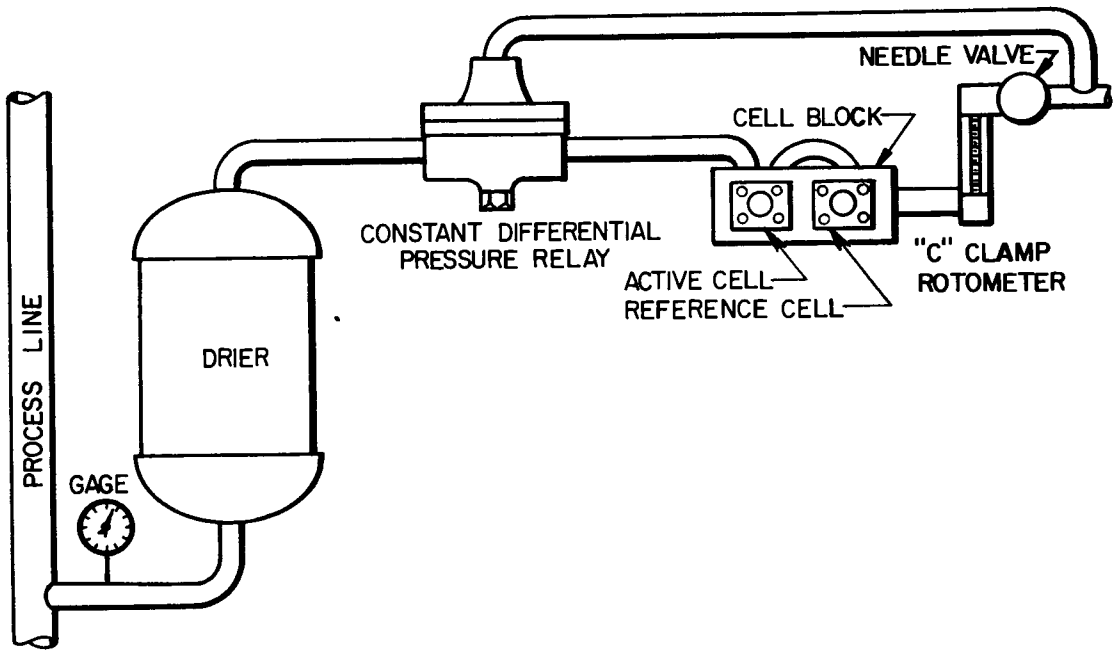

FIGURE 20

SCHEMATIC DIAGRAM OF THE ANALYZER SAMPLING SYSTEM

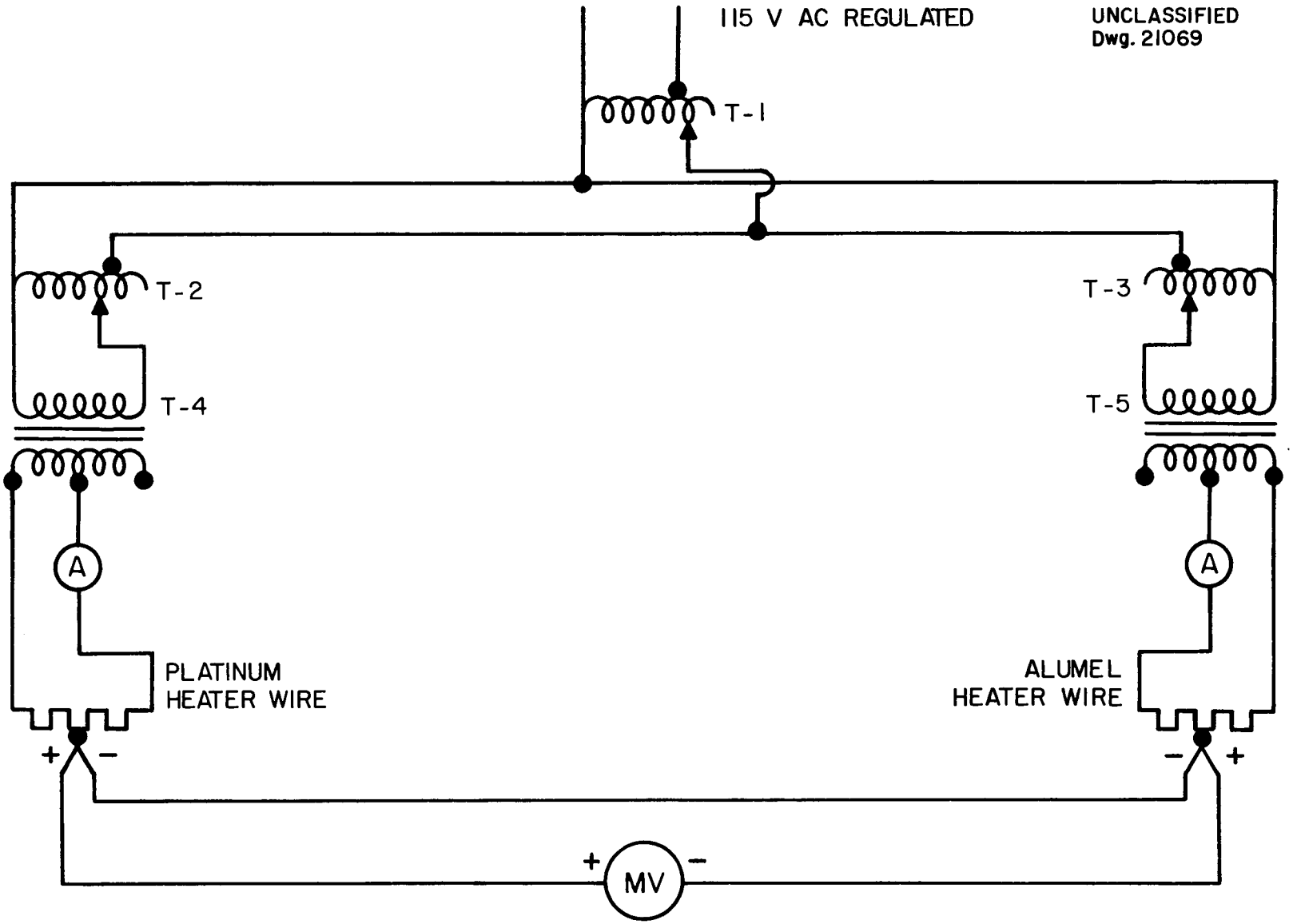

FIGURE 21

SCHEMATIC DIAGRAM OF THE HEATER CURRENT CONTROL

adjusted until the two thermocouples, which are connected in parallel opposition, are at the same temperature with no hydrogen present in the gas stream; with equal wire temperatures, the net output of the thermocouple circuit is zero. When uncombined hydrogen and oxygen are present in the gas stream, the hot platinum wire will catalyze the exothermic recombination reaction of a small amount of the gas and the platinum wire temperature will increase. Since no recombination takes place on the alumel wire, the two thermocouples will be at different temperatures and a millivoltmeter in the thermocouple circuit will indicate the difference in potential between them. This potential is then related to the percentage of hydrogen in the gas by calibrating the analyser with known quantities of gas from an electrolytic cell.

Calibration

Figure 22 is a calibration curve obtained with a total flow of 0.6 CFH through the analyser cells, and a platinum wire current of 3.0 amperes and an alumel wire current of 1.8 amperes. Hydrogen and oxygen gas in a stoichiometric ratio for calibration was obtained from an electrolytic cell consisting of two steel plate electrodes in a 15 percent sodium hydroxide solution. The calibration on such a cell is 0.0037 SCFM of $2H_2 + O_2$ total gas liberated for 10 amperes of direct current through the cell.

For purposes of the calibration, the diluent air stream was passed through the electrolytic cell to reduce the effect of a possible leak. Checks against cell leaks and non-linearity were made by changing both the gas production and diluent air flow, and observing any differences in analyser readings - there were none.

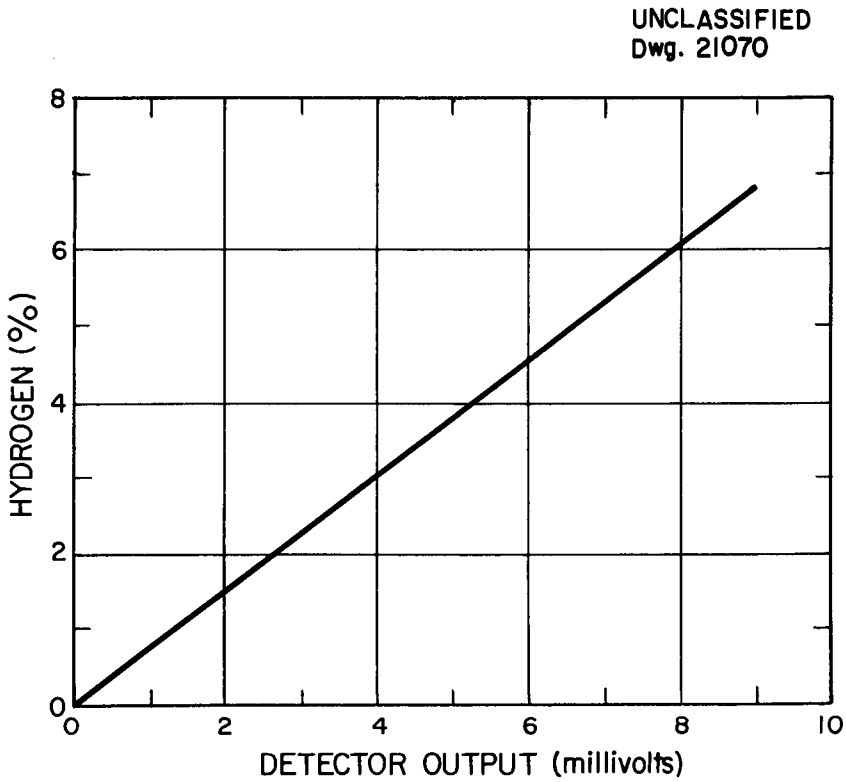

FIGURE 22

A TYPICAL ANALYZER CALIBRATION CURVE

The analyser as described has a useful sensitivity of 1/4 percent hydrogen as determined by drift on weekly checks.

Recorder

The recorder used was a Minneapolis-Honeywell self-balancing potentiometer with a range of 0 to 1 millivolts. The range was extended in one millivolt steps by use of an external suppression circuit.

The platinum cell and cell block were developed by Dr. S. B. Spracklen of the Carbide and Carbon Chemicals Company and are available from the Davis Emergency Equipment Company, Newark, N. J., as Code 11 thermal conductivity units. The alumel reference cell can be fabricated from a platinum cell by replacing the platinum wire with alumel.

Acknowledgment

The authors wish to thank Mr. D. S. Toomb of the Reactor Experimental Engineering Division, Instrumentation Section, Oak Ridge National Laboratory, for permission to use this section of his paper, "A Catalytic Combustion Hydrogen Gas Analyser", and for developing this analyser which proved to be both convenient and dependable.

APPENDIX B

Derivation of the Equation Relating Recombination Efficiency to Hydrogen-Oxygen Ratio

Assume a catalytic bed with uniform lateral mixing, no longitudinal mixing and no channeling. Assume also that diffusion of H_2 and O_2 to the catalyst surface is the only factor determining reaction rate.

A slug of steam containing dilute amounts of H_2 and O_2 enters the bed. The amount of O_2 is slightly in excess of the stoichiometric ratio. Since O_2 is the slower-diffusing gas, it controls the reaction rate in the initial portion of the bed, and its diffusion may be expressed

$$\frac{dO}{d\theta} = -K_o A\Delta O \qquad (1)$$

where

O is the concentration of O_2 in the gas stream

θ is time

K_o is the mass transfer coefficient for O_2

A is the catalyst area in contact with the slug of gas

ΔO is the concentration difference across the film

If it is assumed that the O_2 concentration at the catalyst surface is close to zero, then equation (1) may be written:

$$\frac{dO}{d\theta} = -K_o AO \qquad (2)$$

As the gas passes through the bed, recombination occurs and the hydrogen-oxygen ratio decreases until at some plane 1, hydrogen diffusion begins to control the kinetics. For the remainder of the bed:

$$\frac{dH}{d\theta} = K_H A H \qquad (3)$$

where H replaces O in equation (2).

Integrating equation (2) between entering plane 0 and plane 1, and equation (3) between plane 1 and final plane 2:

$$\ln \frac{O_o}{O_1} = K_o\ A\ \theta_{o-1} \tag{4}$$

$$\ln \frac{H_1}{H_2} = K_H\ A\ \theta_{1-2} \tag{5}$$

where the subscripts o,1,2 refer to the respective planes.

For a system possessing a constant Reynolds number and assumed constant density and viscosity:

$$\frac{K_H}{K_o} = \left(\frac{D_H}{D_o}\right)^n \tag{6}$$

where D_H and D_o are the diffusivities of H_2 and O_2, respectively.

n is an exponent of 0.6 to 0.7, according to the literature.

Substituting (6) into (4), adding (4) and (5), and simplifying by letting $x = \left(\frac{D_H}{D_o}\right)^n$:

$$\frac{x}{K_H A} \ln \frac{O_o}{O_1} + \frac{1}{K_H A} \ln \frac{H_1}{H_2} = \theta_{o-1} + \theta_{1-2} = \theta_t \tag{7}$$

If H_2 diffusion controlled throughout the bed (low H_o/O_o), equation (5) may be written:

$$\ln \frac{H_o^*}{H_2^*} = K_H\ A\ \theta_t \tag{8}$$

where

θ_t is the total time in the bed

H^* refers to hydrogen concentration in a bed where hydrogen diffusion controls throughout

For a given Reynolds number, temperature and pressure, θ_t is a constant, and equating θ_t in (7) and (8):

$$\frac{1}{K_H A} \ln \frac{H_o^*}{H_2^*} = \frac{x}{K_H A} \ln \frac{O_o}{O_1} + \frac{1}{K_H A} \ln \frac{H_1}{H_2}$$

If H_o^*/H_2^* is called f, this simplifies to:

$$\ln \frac{1}{f} = x \ln \frac{O_1}{O_o} + \ln \frac{H_1}{H_2} \tag{9}$$

Furthermore, at plane 1:

$$K_o O_1 = 0.5\ K_H H_1 \text{ or } O_1 = \frac{x}{2} H_1 \tag{10}$$

Also,

$$O_1 = 0.5\ H_1 + O_o - 0.5\ H_o \tag{11}$$

from a material balance.

Combining (9), (10) and (11) and simplifying:

$$\ln \frac{H_2}{2O_o - H_o} = x \ln \frac{O_o}{2O_o - H_o} + \ln \frac{(x-1)^{x-1}}{\left(\frac{x}{2}\right)^x} - \ln f \tag{12}$$

The quantities H_o, O_o and H_2 are measured experimentally. When $\frac{H_2}{2O_o - H_o}$ is plotted against $\frac{O_o}{2O_o - H_o}$ on log-log paper, for a series of constant flow-pressure-temperature runs, a straight line of slope x should be produced. Furthermore when $\frac{H_2}{2O_o - H_o}$ is 1 (logarithm is o), $\frac{H_2}{2O_o - H_o} = \frac{(x-1)^{x-1}}{f\left(\frac{x}{2}\right)^x}$. This allows the evaluation of f, which may be checked experimentally by runs with high excess oxygen.

APPENDIX C

Theoretical Calculation of Recombination with Diffusion Controlling

The method for calculating recombiner efficiency based on diffusion controlling the reaction kinetics is presented in ORNL CF-53-6-162 (I. Spiewak and R. E. Aven, "Design of ISHR Catalytic Recombiner"). This method has been used to predict the behavior of the experimental bed.

The basis of a sample calculation is as follows:

1. Hydrogen diffusion controlling.
2. Temperature of catalyst bed - 800°F.
3. Pressure - 20 psia.
4. Flow of gas plus steam - 11 scfm. = 1.535 lb./sec.ft.^{2}
5. Catalyst bed - 1/8-in. cylindrical pellets, 1.39 in.^{3} bed volume in 1-in. schedule 40 pipe.
6. Gas properties those of steam

   specific volume, 37.5 ft.^{3}/lb.

   viscosity, 1.680×10^{-5} lb./sec.ft.

   diffusion coefficient of H_2 through steam, 3.09×10^{-3} ft.^{2}/sec.

The Reynolds number for these conditions is defined as D_pG/μ, where D_p is pellet diameter, ft; G is mass flow, lb./sec.ft.^{2}, and μ is viscosity, lb./sec.ft.

$$Re = \frac{D_pG}{\mu} = \frac{(1/96)(1.535)}{1.680 \times 10^{-5}} = 952$$

The Chilton-Colburn dimensionless parameter is calculated as follows:

$$j_D = 0.99\ (Re)^{-0.41} = 0.0594$$

The mass transfer coefficient, K_G, is:

$$K_G = j_D \frac{G}{M\ P_f} \left(\frac{\rho D}{\mu}\right)^{2/3} = (.0594)\frac{(1.535)}{(18)(20)}\left[\frac{(1/37.5)(3.09 \times 10^{-3})}{1.68 \times 10^{-5}}\right]^{2/3} \qquad (1)$$

$$K_G = 7.29 \times 10^{-4} \frac{\text{lb. mol}}{\text{sec. ft.}^2 \text{ psi.}}$$

where M is average molecular weight of gas stream

P_f is gas pressure, psi.

ρ is gas density, lb./ft.^{3}

D is diffusion coefficient ft.^{2}/sec.

The equation describing the mass transfer is:

$$\frac{\Delta H}{\Delta t} = K_G A\ \Delta f_{LM} \qquad (2)$$

where $\Delta H/\Delta t$ is moles of hydrogen transferred per second

A is the catalyst area in the bed

Δf_{LM} is the log mean driving force expressed as mol fraction hydrogen in gas stream

The amount of hydrogen transferred per second is also equal to the total gas flow rate times the change in hydrogen concentration going through the bed. Therefore, modifying equation (2):

$$\frac{\Delta H}{\Delta t} = m\ (f_1 - f_2) = K_G A \frac{(f_1 - f_2)}{\ln f_1/f_2}$$

$$\ln f_1/f_2 = \frac{K_G A}{m} \qquad (3)$$

where f_1, f_2 are mol fractions of H_2 in and out of bed

m is gas flow rate, lb. mol./sec.

Substituting into equation (3)

$$K_G = 7.29 \times 10^{-4} \frac{\text{mol.}}{\text{sec.ft.}^2\text{psi.}} = 1.46 \times 10^{-2} \frac{\text{mol.}}{\text{sec.ft.}^2\text{(mol.fraction)}}$$

$A = 0.278$ ft.^{2} for catalyst bed

$m = 5.1 \times 10^{-4}$ lb. mol./sec.

$$f_1/f_2 = 2850$$

This ratio has been defined as f in the body of the report.

The theoretical amount of mass transfer for a given mass flow rate and composition is independent of pressure. The variation in K_G with temperature between the limits 400°F and 1000°F is only 12%.

APPENDIX D

Table of Observed Mass Transfer Coefficients

Temperature °C.	Pressure psia.	Total Flow Rate scfm	Controlling Diffusant	Coefficient $\frac{\text{lb. mol.}}{\text{sec. ft.}^2\text{(mol.fraction)}}$
232	80	16.27	Hydrogen	2.70×10^{-3}
243	100	16.45	Hydrogen	2.52×10^{-3}
222	50	16.15	Hydrogen	2.63×10^{-3}
285	30	16.23	Hydrogen	2.65×10^{-3}
296	50	16.3	Hydrogen	3.01×10^{-3}
302	80	16.25	Hydrogen	3.10×10^{-3}
425	35	16.15	Hydrogen	4.97×10^{-3}
435	50	16.15	Hydrogen	5.38×10^{-3}
432	80	16.0	Hydrogen	5.98×10^{-3}
434	100	15.95	Hydrogen	6.44×10^{-3}
423	30	13.33	Hydrogen	4.87×10^{-3}
438	50	13.27	Hydrogen	5.34×10^{-3}
439	80	13.27	Hydrogen	5.73×10^{-3}
427	110	13.2	Hydrogen	5.77×10^{-3}
516	80	12.98	Hydrogen	6.14×10^{-3}
516	100	13.08	Hydrogen	6.18×10^{-3}
507	30	13.17	Hydrogen	4.66×10^{-3}
522	50	13.17	Hydrogen	5.73×10^{-3}
347	50	13.17	Hydrogen	4.69×10^{-3}
342	30	13.27	Hydrogen	4.08×10^{-3}
348	80	13.23	Hydrogen	4.03×10^{-3}
351	110	13.3	Hydrogen	5.19×10^{-3}
233	30	13.33	Hydrogen	2.38×10^{-3}
231	50	13.3	Hydrogen	2.19×10^{-3}
229	80	13.33	Hydrogen	2.15×10^{-3}
230	100	13.4	Hydrogen	2.08×10^{-3}
401	50	9.06	Hydrogen	3.51×10^{-3}
400	50	13.7	Hydrogen	4.38×10^{-3}
396	50	17.1	Hydrogen	4.88×10^{-3}
400	50	20.0	Hydrogen	5.12×10^{-3}
397	50	23.6	Hydrogen	5.48×10^{-3}

APPENDIX D (CONT'D)

Table of Observed Mass Transfer Coefficients

Temperature °C	Pressure psia.	Total Flow Rate scfm	Controlling Diffusant	Coefficient lb. mol. / sec.ft.^{2}(mol.fraction)
398	100	8.81	Hydrogen	3.68×10^{-3}
401	100	12.2	Hydrogen	4.60×10^{-3}
399	100	16.2	Hydrogen	5.78×10^{-3}
396	100	18.7	Hydrogen	6.31×10^{-3}
395	100	20.8	Hydrogen	6.57×10^{-3}
398	100	23.3	Hydrogen	6.89×10^{-3}
396	100	21.8	Hydrogen	6.73×10^{-3}
400	100	16.4	Hydrogen	5.33×10^{-3}
401	100	12.7	Hydrogen	4.53×10^{-3}
395	100	8.25	Hydrogen	3.73×10^{-3}
405	100	14.8	Hydrogen	4.97×10^{-3}
401	100	12.0	Hydrogen	4.41×10^{-3}
399	100	18.1	Hydrogen	5.80×10^{-3}
401	100	8.05	Hydrogen	3.59×10^{-3}
350	50	9.61	Hydrogen	3.52×10^{-3}
350	50	9.60	Oxygen	2.05×10^{-3}
350	50	9.74	Deuterium	2.58×10^{-3}

APPENDIX E

Summary of Observed and Calculated Data

Date	Inlet Flow Rate, scfm H_2O	H_o	O_o	Pressure psia	Temperature, °C Inlet	Bed	Outlet	Efficiency %	H_f, Unrecombined Hydrogen scfm	$\frac{H_f}{2O_o-H_o}$	$\frac{O_o}{2O_o-H_o}$
April 15	12.1	.591	.546	50	147	352	346	87.9	.0717	.143	1.09
	12.1	.585	.462	50	147	348	340	85.8	.0830	.244	1.36
	12.1	.580	.416	50	148	340	332	83.6	.0950	.377	1.65
	12.1	.629	.448	30	145	332	330	78.0	.139	.520	1.67
	12.2	.629	.512	30	142	344	338	81.6	.115	.292	1.30
	12.1	.629	.550	30	142	350	341	83.2	.106	.225	1.17
	12.2	.574	.555	80	151	349	342	89.6	.0595	.111	1.03
	12.2	.579	.477	80	152	350	345	87.9	.0702	.187	1.27
	12.1	.579	.426	80	152	345	342	86.4	.0789	.289	1.56
	12.2	.579	.417	110	163	349	333	86.9	.0758	.297	1.63
	12.2	.580	.486	110	163	351	334	89.2	.0625	.160	1.24
	12.2	.580	.570	110	163	353	334	90.2	.0567	.101	1.02
April 16	11.8	.842	.723	30	139	435	409	86.9	.110	.183	1.20
	11.8	.842	.616	30	140	421	409	82.8	.145	.372	1.58
	11.9	.863	.578	30	142	412	411	78.4	.186	.635	1.97
	11.8	.851	.552	50	145	435	430	84.5	.132	.521	2.18
	11.8	.832	.626	50	146	441	432	88.3	.0970	.231	1.49
	11.8	.798	.718	50	145	439	430	90.5	.0756	.119	1.13
	11.8	.778	.718	80	152	445	440	92.3	.0596	.0906	1.09
	11.8	.780	.630	80	152	439	430	91.2	.0683	.142	1.31
	11.8	.780	.569	80	152	434	426	90.3	.0772	.215	1.59

APPENDIX E (CONT'D)

Date	Inlet Flow Rate, scfm H_2O	H_o	O_o	Pressure psia	Temperature, °C Inlet	Bed	Outlet	Efficiency %	H_f, Unrecombined Hydrogen scfm	$\frac{H_f}{2O_o-H_o}$	$\frac{O_o}{2O_o-H_o}$
	11.8	.800	.591	110	165	427	421	90.5	.0758	.199	1.55
	11.7	.805	.645	110	164	430	422	91.6	.0676	.140	1.33
	11.7	.800	.716	110	165	425	420	92.5	.0601	.0950	1.13
April 21	11.2	.887	.883	100	159	518	488	94.3	.0508	.0579	1.01
	11.5	.953	.767	100	159	515	487	93.3	.0639	.110	1.32
	11.3	.935	.703	100	150	515	487	92.7	.0680	.145	1.50
	11.4	.945	.691	80	149	509	475	87.4	.119	.273	1.59
	11.3	.928	.712	80	153	519	490	92.5	.0697	.141	1.44
	11.4	.915	.763	80	152	519	490	93.9	.0562	.0916	1.25
	11.4	.912	.858	80	150	518	490	94.6	.0495	.0614	1.06
April 22	11.4	.984	.781	30	141	508	480	86.9	.129	.219	1.33
	11.4	.951	.854	30	141	501	479	87.9	.115	.152	1.13
	11.4	1.01	.720	30	142	511	488	85.3	.148	.338	1.64
	11.4	.995	.713	50	146	522	500	88.9	.110	.256	1.65
	11.4	.972	.772	50	146	522	500	90.8	.0895	.157	1.35
	11.5	.964	.875	50	145	521	500	92.4	.0731	.092	1.11
	11.3	.892	.848	80	151	511	490	94.7	.0472	.0586	1.00
	11.3	.883	.698	80	151	509	484	93.5	.0571	.111	1.36
	11.3	.882	.657	80	152	508	482	92.6	.0654	.151	1.52
	11.5	.910	.658	100	160	505	470	92.3	.0705	.173	1.62
	11.5	.900	.784	100	160	510	470	94.2	.0520	.0780	1.18
April 23	12.7	.346	.330	30	144	242	233	65.5	.120	.382	1.05
	12.7	.346	.300	30	144	235	230	61.9	.132	.520	1.18
	12.7	.345	.274	30	145	223	224	58.4	.144	.696	1.32

APPENDIX E (CONT'D)

Date	Inlet Flow Rate, scfm H_2O	H_o	O_o	Pressure psia	Temperature, °C Inlet	Bed	Outlet	Efficiency %	H_f, Unrecombined Hydrogen scfm	$\frac{H_f}{2O_o-H_o}$	$\frac{O_o}{2O_o-H_o}$
	12.7	.328	.269	50	149	229	226	60.0	.131	.624	1.28
	12.7	.327	.309	50	149	233	228	62.4	.123	.421	1.06
	12.7	.313	.276	80	154	225	227	59.7	.126	.527	1.16
	12.6	.365	.276	80	154	227	229	58.7	.151	.810	1.48
	12.6	.346	.327	80	154	235	230	62.1	.131	.425	1.06
	12.7	.359	.316	100	160	230	235	60.4	.142	.520	1.16
	12.7	.359	.355	100	160	230	230	60.4	.142	.405	1.01
April 24	15.2	.576	.483	80	155	233	255	62.0	.219	.561	1.24
	15.2	.576	.443	80	156	231	254	60.4	.228	.735	1.45
	15.2	.571	.522	80	155	233	258	63.1	.211	.445	1.10
	15.3	.588	.515	100	161	245	263	63.7	.213	.482	1.17
	15.4	.602	.475	100	160	240	261	62.3	.227	.630	1.37
	15.1	.580	.488	50	150	225	250	59.9	.233	.588	1.23
	15.1	.575	.439	50	149	218	240	56.2	.252	.831	1.45
April 28	14.8	.781	.570	30	143	275	275	58.7	.322	.895	1.58
	14.8	.767	.631	30	142	287	275	62.6	.286	.578	1.28
	14.8	.785	.689	30	142	292	289	61.6	.302	.511	1.17
	14.9	.737	.635	50	149	302	298	67.7	.238	.446	1.19
	15.0	.735	.567	50	149	295	290	65.4	.254	.627	1.42
	15.0	.811	.514	50	149	290	280	59.7	.327	1.51	2.36
	14.9	.746	.514	80	155	295	296	64.8	.262	0.93	1.82
	15.0	.735	.586	80	155	310	304	68.0	.235	.536	1.34
April 30	14.2	1.04	.855	35	142	422	400	83.2	.174	.260	1.27
	14.3	1.18	.736	35	144	429	410	73.8	.309	1.06	2.52

APPENDIX E (CONT'D)

Date	Inlet Flow Rate, scfm H_2O	H_o	O_o	Pressure psia	Temperature, °C Inlet	Bed	Outlet	Efficiency %	H_f, Unrecombined Hydrogen scfm	$\frac{H_f}{2O_o-H_o}$	$\frac{O_o}{2O_o-H_o}$
	14.4	1.12	.703	50	148	435	420	78.9	.236	.833	2.48
	14.3	.986	.780	50	148	435	422	84.5	.152	.265	1.36
	14.3	.911	.773	80	154	431	421	89.0	.101	.158	1.21
	14.3	.960	.691	80	154	432	426	85.6	.138	.327	1.64
	14.3	.919	.746	100	160	432	422	89.9	.0927	.161	1.30
	14.3	.976	.660	100	159	437	426	85.9	.138	.400	1.92
May 19	9.06	.312	.322	50	151	352	320	89.0	.0344	.970	.104
	9.06	.314	.263	50	152	352	319	88.2	.0372	1.24	.175
	9.06	.314	.211	50	153	350	315	85.1	.0469	1.95	.434
	9.06	.314	.242	50	153	352	320	87.2	.0402	1.43	.236
	9.06	.314	.226	50	153	351	318	86.4	.0428	1.64	.310
	9.06	.326	.198	50	153	349	314	81.5	.0601	2.83	.859
	9.06	.355	.183	50	153	348	315	75.2	.0879	16.7	8.0
	9.06	.330	.196	50	153	350	314	81.0	.0627	3.16	1.01
	9.06	.308	.348	50	152	348	310	89.7	.0315	0.898	0.0813
	9.06	.308	.506	50	150	345	315	89.6	.0320	0.718	0.0454
May 22 Deuterium Runs	9.08	.329	.326	50	150	350	295	79.5	.0676	.209	1.01
	9.06	.329	.279	50	152	352	310	79.6	.0671	.293	1.22
	9.08	.333	.248	50	152	350	308	75.8	.0805	.494	1.52
	9.06	.342	.222	50	153	345	303	70.8	.100	.980	2.18
	9.06	.344	.237	50	152	348	304	72.2	.955	.735	1.82

APPENDIX E (CONT'D)

Date	Inlet Flow Rate, scfm H_2O	H_o	O_o	Pressure psia	Temperature, °C Inlet	Bed	Outlet	Efficiency %	H_f, Unrecombined Hydrogen scfm	H_o/H_f
May 11	8.3	.369	.387	50	150	401	370	90.2	.0361	10.22
	12.5	.620	.576	50	153	400	379	85.3	.0912	6.80
	15.6	.752	.755	50	155	396	376	81.9	.136	5.53
	18.2	.906	.876	50	155	400	379	78.4	.196	4.62
	21.4	1.11	1.06	50	154	379	372	75.1	.276	4.02
May 12	8.1	.335	.370	100	156	398	350	91.8	.0276	12.14
	11.2	.516	.529	100	159	401	354	89.6	.0538	9.58
	14.8	.681	.712	100	162	399	365	88.3	.0800	8.51
	17.1	.780	.843	100	162	396	375	86.7	.1040	7.50
	19.0	.864	.918	100	162	395	368	84.9	.130	6.65
	21.2	1.02	1.05	100	162	398	371	83.0	.173	5.89
May 5	19.6	1.16	1.04	100	158	396	382	84.3	.182	6.37
	14.8	.823	.800	100	157	400	378	85.8	.117	7.03
	11.5	.644	.598	100	159	401	369	88.3	.0755	8.53
	7.5*	.358	.395	100	159	395	360	93.4	.0237	15.12
May 7	13.3	.794	.744	100	158	405	382	86.6	.106	7.49
	10.8	.628	.614	100	158	401	369	88.9	.0697	9.01
	16.3	.922	.928	100	157	399	379	85.4	.135	6.83
	7.3*	.354	.395	100	158	401	362	93.1	.0245	14.45

* Steam flow rate calculated from recombiner temperature because of condensation in steam orifice.

[redacted]

[redacted]